

ISTANBUL TECHNICAL UNIVERSITY ★ INFORMATICS INSTITUTE

**A BLOCK PROCESSING APPROACH FOR DOPPLER CENTROID
ESTIMATION**

M.Sc. THESIS

Pelin TUNÇAY

Department of Communication Systems

Satellite Communication and Remote Sensing Programme

JUNE 2013

ISTANBUL TECHNICAL UNIVERSITY ★ INFORMATICS INSTITUTE

**A BLOCK PROCESSING APPROACH FOR DOPPLER CENTROID
ESTIMATION**

M.Sc. THESIS

**Pelin TUNÇAY
(705101008)**

Department of Communication Systems

Satellite Communication and Remote Sensing Programme

Thesis Advisor: Assoc. Prof. Dr. Mesut KARTAL

JUNE 2013

İSTANBUL TEKNİK ÜNİVERSİTESİ ★ BİLİŞİM ENSTİTÜSÜ

DOPPLER MERKEZİ KESTİRİMİ İÇİN BLOK İŞLEME YAKLAŞIMI

YÜKSEK LİSANS TEZİ

**Pelin TUNÇAY
(705101008)**

İletişim Sistemleri Anabilim Dalı

Uydu Haberleşmesi ve Uzaktan Algılama Programı

Tez Danışmanı: Doç. Dr. Mesut KARTAL

HAZİRAN 2013

Pelin Tunçay, a **M.Sc.** student of ITU **Institute of Informatics** student ID **705101008**, successfully defended the **thesis** entitled “**A BLOCK PROCESSING APPROACH FOR DOPPLER CENTROID ESTIMATION**”, which she prepared after fulfilling the requirements specified in the associated legislations, before the jury whose signatures are below.

Thesis Advisor : **Assoc. Prof. Dr. Mesut KARTAL**

İstanbul Technical University

Jury Members : **Prof. Dr. Sedef KENT**

İstanbul Technical University

Prof. Dr. Osman Nuri UÇAN

İstanbul Aydın University

Date of Submission : 03 May 2013

Date of Defense : 06 June 2013

To my spouse and my family,

FOREWORD

I would like to thank my advisor, Assoc. Prof. Dr. Mesut KARTAL, and declare my gratitude for all the support and knowledge he has provided me since the day I've started my Masters degree.

In particular, I would like to thank my husband for his love and patience during the periods I spent most of the time on my work and for his understanding as to my absence from home.

I also would like to thank my parents for having faith in my will and success, and being supportive and reassuring at all times.

June 2013

Pelin TUNÇAY
(Electrical and Electronics
Engineer)

TABLE OF CONTENTS

	<u>Page</u>
FOREWORD	ix
TABLE OF CONTENTS	xi
ABBREVIATIONS	xiii
LIST OF TABLES	xv
LIST OF FIGURES	xvii
SUMMARY	xix
ÖZET	xxi
1. INTRODUCTION	1
1.1 Purpose of Thesis	4
1.2 Literature Review	4
1.2.1 SAR resolution	4
1.2.2 SAR signal properties	5
1.2.3 Azimuth aliasing	7
1.2.4 Doppler centroid	8
1.2.5 Range cell migration	9
1.3 Range Doppler Algorithm	9
1.4 Doppler Centroid Estimation	16
1.4.1 Doppler centroid calculation from geometry	17
1.5 Baseband Doppler Centroid Estimation	17
1.5.1 Magnitude based Doppler centroid estimation approach.....	17
1.5.2 Phase based Doppler centroid estimation approach.....	19
1.6 Doppler Ambiguity Resolver (DAR)	20
1.6.1 Magnitude based DAR estimation method	20
1.6.2 Phase based DAR estimation method	20
1.7 Hypothesis	23
2. EXPERIMENTAL RESULTS	25
3. CONCLUSIONS AND RECOMMENDATIONS	35
REFERENCES	37
CURRICULUM VITAE	39

ABBREVIATIONS

ACCC	: Average Cross Correlation Coefficient
DAR	: Doppler Ambiguity Resolver
DLR	: German Aerospace Center
FFT	: Fast Fourier Transform
FM	: Frequency Modulation
IFFT	: InverseFast Fourier Transform
MLBF	: Multi-Look Beat Frequency
MLCC	: Multi-Look Cross Correlation
PRF	: Pulse Repetition Frequency
PRI	: Pulse Repetition Interval
RCM	: Range Cell Migration
RCMC	: Range Cell Migration Correction
RDA	: Range Doppler Algorithm
SAR	: Synthetic Aperture Radar
SNR	: Signal to Noise Ratio
WDA	: Wavelength Diversity Algorithm

LIST OF TABLES

	<u>Page</u>
Table 2.1 : RADARSAT-1 parameters.	25

LIST OF FIGURES

	<u>Page</u>
Figure 1.1 : SAR geometry.	2
Figure 1.2 : Antenna beamwidth and synthetic aperture.	3
Figure 1.3 : Transmit and receive cycles	5
Figure 1.4 : Azimuth beam pattern and its effect on azimuth signal.	6
Figure 1.5 : Presentation of the azimuth aliasing caused by PRF sampling.	8
Figure 1.6 : RDA algorithm overview	10
Figure 1.7 : Simulation of raw data with no squint case.	12
Figure 1.8 : Range compressed data (no squint case).	13
Figure 1.9 : Final image after azimuth compression (no squint case)	13
Figure 1.10 : Simulation of raw data which has a 10o squint angle.	14
Figure 1.11 : Range compressed data (squint case).	14
Figure 1.12 : Final image that processed with a -90 Hz Doppler centroid	15
Figure 1.13 : Final image that processed with zero Doppler centroid	15
Figure 1.14 : Magnitude based Doppler centroid estimation approach	18
Figure 2.1 : Raw data of the Vancouver Airport.	26
Figure 2.2 : Range domain matched filter.	26
Figure 2.3 : Range compressed data.	27
Figure 2.4 : Doppler centroid estimation result.	27
Figure 2.5 : Azimuth domain matched filter.	28
Figure 2.6 : Final image	28
Figure 2.7 : Stanley Park region.	29
Figure 2.8 : Brackendale region.	29
Figure 2.9 : The region of English Bay ships.	30
Figure 2.10 : Obtained image from whole data (Vancouver city).	31
Figure 2.11 : Unseen targets.	32
Figure 2.12 : Doppler centroid errors.	33

A BLOCK PROCESSING APPROACH FOR DOPPLER CENTROID ESTIMATION

SUMMARY

Synthetic Aperture Radar (SAR) is a type of imaging radar, which uses signal-processing techniques to obtain finer resolution. The most commonly used algorithm to create an image from raw data in strip map mode SAR is the Range Doppler Algorithm (RDA). It is based on pulse compression techniques. If the compression process is not done correctly, signal to noise ratio (SNR) would reduce, and image misregistration and geometric distortions would be occurred. In RDA, frequency domain matched filter is used for pulse compression. Defining a matched filter is simple in range domain. Because the filter parameter can be derived from the transmitted signal. However, for azimuth domain matched filter, the parameters cannot be derived. The received signal is shifted because of sensor motion. This situation is called Doppler shift. To find the amount of the shift Doppler centroid frequency must be known.

Doppler centroid can be calculated from the SAR geometry. In satellite SAR, orbit and attitude information is necessary. However, accurate orbit geometry information cannot be always provided. In airborne SAR, the undesired aircraft motions usually caused by weather condition do not allow to obtain accurate geometric information. Furthermore, scene contents such as landforms, buildings etc. also affect the geometry calculations. Estimating Doppler centroid from the received data is a well-known technique. There are a lot of studies in the literature on this topic. Doppler centroid is composed of two parts according to their usage: the fractional part and the integer part. The fractional part is also defined as the baseband Doppler centroid, which is used for azimuth compression. The integer part, which is called as the ambiguity part, is necessary for range cell migration correction (RCMC). Therefore, Doppler centroid estimation is done separately for each part.

In order to estimate baseband Doppler centroid, two methods are used in the literature. One of them is magnitude-based estimator. In this algorithm, power spectrum of the azimuth signal gives a solution for baseband Doppler centroid. The spectrum is observed at one Pulse Repetition Frequency (PRF) range within the $[-PRF/2, PRF/2]$. Then, the frequency at where the peak of the spectrum occurs gives the Doppler centroid frequency. The other method is phase-based estimator, which is based on the calculation of the average cross correlation coefficient (ACCC) between the azimuth samples.

Existing algorithms work well with the different types of scene with some assumptions. Since the Doppler centroid is estimated using the data of the whole scene, some distortions occur in the final image away from the Doppler centroid.

In this work, we propose an alternative method based on block processing to eliminate the distortions in the final image. In proposed method, the scene is divided

into many sub-scenes, and then the RDA is applied to each of those sub-scenes. The Doppler centroid estimation and azimuth compression is done separately for each sub-scene.

DOPPLER MERKEZİ KESTİRİMİ İÇİN BLOK İŞLEME YAKLAŞIMI

ÖZET

Sentetik açıklıklı radarlar (SAR), sinyal işleme algoritmalarını kullanarak yüksek çözünürlüklü görüntü elde eden görüntüleme radarlarıdır. Çözünürlük, diğer bir deyişle yerdeki hedeflerin ayırılabilirliği, iki şekilde ifade edilir. Bunlar hareket doğrultusundaki çözünürlük (azimut çözünürlük) ve bu yöne çapraz olan menzil çözünürlüğüdür. Radar sistemlerinde yüksek çözünürlük elde etmek için, menzil yönünde, darbe sıkıştırma yöntemi kullanılır. Darbe süresindeki kısalma daha iyi menzil çözünürlüğü sağlar. Darbe süresini kısaltmanın bazı limit değerleri vardır. Burada, sinyalin gönderilip geri alınabilmesi için gücün belli bir değerin üzerinde olması gerekir. Sinyal gürültü oranı da hesaba katılmalıdır. Menzil çözünürlüğü bütün radar sistemleri için aynıdır. SAR sistemini diğer radar sistemlerinden ayıran özelliği, hareket doğrultusundaki çözünürlüktür. Bu yöndeki çözünürlüğü iyileştirmek için anten boyunun uzun olması gereklidir. Uzun anten boyu, her ne kadar yer radarlarında elde edilebilir olsa da, kullanımı verimli değildir. Özellikle bir platform üzerine yerleştirildiğinde, bu platformu taşıyacak olan uçak veya uydunun kapasitesi yetersiz kalacaktır. SAR sistemi faz dizili antene benzer şekilde çalışır. Ancak burada çok sayıda anten elemanı kullanılmaz. SAR sisteminde uzun anten boyu, sinyal işleme algoritmaları kullanılarak sentezlenir. Değişik anten konumları sensörün hareketiyle sağlanır. Bu sentezleme işlemi için, daha kısa anten boyu gereklidir. SAR sisteminde, iki nokta arasındaki uçuş sırasında, her gönderilen darbenin yansımalarının genlikleri ve fazları kaydedilir. Bu verilerden faydalanılarak, çok daha uzun anten boyu ile elde edilebilecek çözünürlükteki görüntü oluşturulabilir.

SAR sistemleri farklı modlarda çalışır. Bunlar, tarama modu, şerit görüntüleme modu ve spot ışıklandırma modu olarak adlandırılır. Bu çalışmada şerit görüntüleme modu kullanılmıştır. Bu tip SAR sistemleri, platformun ana ekseninden geçen yeryüzüne dik olan düzlemde değil, bu düzlemler arasında belli bir açı olacak şekilde, eğik aşağı ya da yukarı doğru bakarak görüntü alırlar. Şerit görüntüleme radarlarında, ham veriden görüntü oluşturmak için kullanılan en yaygın algoritma Range (menzil) Doppler Algoritması'dır (RDA). Bu algoritma, darbe sıkıştırma yöntemine dayanır. Sıkıştırma işlemleri frekans bölgesinde yapılır.

SAR sistemlerinde gönderilen sinyal, lineer frekans modüleli (FM) sinyaldir. Alınan ham SAR verisi, iki boyutlu matris olarak kaydedilir. Satırlar, sensör belli bir pozisyondayken alınan menzil değerleridir. Sütun değerleri ise sensörün hareketini gösterir. Başka bir deyişle, SAR sensörünün hareketi darbe tekrarlama frekansıyla (DTF) örneklenir. Satır değerlerine menzil, sütun değerlerine azimut sinyali denilir.

RDA algoritmasında darbe sıkıştırması yapmak için uyumlu filtreler kullanılır. Bu filtreler menzil ve azimut sinyali için frekans bölgesinde ayrı ayrı tasarlanır. Uyumlu filtreleri tasarlamak için bazı parametrelerin bilinmesi gerekir. Bu parametreler,

alınan sinyalin frekans bölgesindeki bant genişliği ve merkez frekansıdır. Menzil sinyali için bu veriler, gönderilen sinyalden bilinmektedir. Azimut sinyali için bu parametrelerin bulunması daha karışıktır. Alınan sinyal Doppler etkisinden dolayı kaymıştır. Bunun nedeni platformun hareketinden dolayı sensörün hedefe göre bağlı hızı değişir ve bu da frekans etkiler. Azimut sinyalinin merkez frekansının hesap edilmesi önemlidir. Bu frekans, Doppler merkez frekansı olarak adlandırılır ve SAR sinyal işlemede kullanılan önemli bir parametredir.

Doppler merkezi SAR geometrisinden hesap edilebilir. Bunun için, sensörün konumu, yüksekliği ve hızı bilinmelidir. Bu bilgilere ulaşmak her zaman mümkün değildir. Uçakla taşınan SAR sistemlerinde, uçağın konumu, hızı sabit değildir. Hava koşulları, yeryüzü şekillerinin engebeli olması, uçağın düzgün bir doğrultuda gitmesini engelleyebilir. Uydu üzerinde taşınan SAR sistemlerinde, hareket dengeleme sistemleri, sensörün hızını, ve konumunu olabildiğince sabitlemektedir. Ancak Doppler merkezi aynı zamanda yeryüzü şekillerine de bağlıdır. Çünkü Doppler merkez frekansı hedef ile sensör arasındaki mesafeyle ilişkilidir. Bu yüzden, dağlık bir alandaki Doppler merkezi ile yükseltisi daha az olan bir bölgenin Doppler merkezi aynı olmayacaktır. Doppler merkezinin alınan veriden kestirimi çok yaygın bir metottür. Literatürde, bu konu üzerinde yapılmış birçok çalışma bulunmaktadır.

Doppler kestirim yöntemleri iki başlıkta toplanmaktadır. Bunlar, temel bant Doppler merkezi kestirimi ve belirsizlik sayısı kestirimidir. Azimut sinyali darbe tekrarlama frekansıyla örneklenir ve bu durum Nyquist örnekleme kriterini sağlamaz. Çünkü azimut sinyalinin bant genişliği limitsizdir. Bu anten paterninin ana lobun dışında da ilerlemesinden kaynaklanır. Darbe tekrarlama frekansını belirlemesi sadece azimut sinyaline bağlı değildir. Antenin alışı penceresine, yakın ve uzak menzil değerlerine de bağlıdır. Bundan dolayı DTF ile örneklenen azimut sinyali, bozulur ve kendini tekrar eder. Doppler merkezinin bir DTF içinde kalan kısmına kesirli veya temel bant Doppler merkezi denilir. Gerçek Doppler merkezinin hangi tekrar içinde olduğu ise belirsizlik sayısı olarak adlandırılır. Gerçek Doppler merkezi bulunmak isteniyorsa, bu iki kısmın kestirimi ayrı ayrı yapılır. Azimut yönündeki sıkıştırma işlemi için temel bant Doppler merkezinin kestirimi yeterlidir. Eğer ki menzil hücre göçü düzeltme işlemi yapılacaksa iki kısmında bilinmesi gereklidir.

Temel bant Doppler merkezinin alınan veriden kestirimi için literatürde 2 yaklaşım kullanılmaktadır. Bunlardan birisi genlik temelli kestirim, diğeri ise faz temelli kestirimdir. Genlik temelli kestirimde, azimut sinyalinin güç spektrumuna bakılır. Azimut sinyalinin güç spektrumu, anten paterninin yerdeki nokta hedeften yansıyan sinyalle konvolüsyonudur. Anten paterninin maksimum noktasına denk gelen frekans değeri Doppler merkezini verir. Bundan dolayı güç spektrumundan anten paterni kestirilmeye çalışılır. Öncelikle azimut sinyali üzerinde Fourier dönüşümü uygulanır ve güç spektrumu hesaplanır. Tek bir menzil değeri için hesaplanan spektrum anlamsızdır. Ancak diğer menzil değerlerinin spektrumları toplanırsa, ortalama alma işlemi ile Gauss eğrisine benzer bir spektrum elde edilir. Ortalaması alınmış spektrum alçak geçiren filtreden geçirildiğinde, yüksek frekanslı gürültü ve hedeften yansıyan sinyaller bastırılır ve yavaş değişen anten paterni elde edilir. Bu paternin maksimum noktasının frekans değeri Doppler merkez frekansını verir. Bu işlem bazı çalışmalarda ham veri üzerinde uygulanırken, bazı çalışmalarda ise menzil sıkıştırılması yapılmış veri üzerinde uygulanmıştır. Faz temelli kestirimde ise iki azimut örneği arasındaki faz farkı bu yöntemin temelini oluşturur. Bu yöntemde faz artışı da denir. Azimut örnekleri arasındaki ortalama çapraz korelasyon katsayısı hesaplanır. Bu katsayının açısı temel bant Doppler merkezi ile doğru orantılıdır.

Literatürdeki çalışmalar, Doppler kestirimini verimli bir şekilde gerçekleştirmektedir. Ancak görüntünün merkezinden uzaklaştıkça, görüntüde bozulmalar meydana gelmektedir. Bunun sebebi, Doppler merkezinin tüm veri seti için hesaplanmasıdır. Bu durumda Doppler merkezi tüm veri için ortalama bir değer alır. Bu tezde yapılan çalışma alternatif bir yöntem olup, bu hataları olabildiğince en aza indirger. Metot, veri setini parçalara bölerek ayrı ayrı işleme ilkesine dayanır. Böylece, her alt bölgenin merkezi ayrı hesaplanacağından dolayı doğruluğu daha yüksek olan bir kestirim yapılabilecektir. Bu yöntemde, öncelikle ham veri uygun parçalara ayrılır. Menzil Doppler algoritması her parça için ayrı ayrı uygulanır. Her parça, kestirimi yapılan kendi Doppler merkeziyle işlenir.

Bu yöntemin en önemli özelliği, tüm veri işlendiğinde görüntünün merkezinden uzakta olan kısımlarda görünmeyen hedeflerin, o bölgeye ait verinin alt bölgesi işlendiğinde görünür hale gelmesidir. Diğer önemli özelliği ise işleme yükünün azalmasıdır. Bütün veri işlendiğinde işleme süresi çok uzundur. Ancak verinin boyutları küçüldüğünde işleme süresi kısalmıştır. Eğer ki bölgenin tamamı ile ilgilenilmiyorsa, daha ufak bir kısmıyla ilgileniliyorsa, bütün veriyi işlemeye gerek kalmayacaktır. Daha kısa bir sürede, ihtiyaç duyulan alan işlenerek hem zamandan tasarruf edilir hem de doğruluğu daha iyi olan görüntü elde edilir.

Bu yöntemde en çok dikkat edilmesi gereken kısım, alt bölgelerin seçimidir. Aynı yükselti grubuna ait olan kısımlardan bir alt bölge oluşturulabilir. Örneğin, dağlık bir alan ile deniz bölgesi birlikte alınır, burada kestirimi yapılan Doppler merkezi iki alan için de doğru sonuç vermeyecektir. Düzeltilmeye çalışılan kısımlar, bu etkiden dolayı daha çok bozulabilirler. Bu yüzden, dağlık alanları, yerleşim bölgelerini, su ve deniz gibi alanları mümkün olduğunca ayrı parçalarda işlemek en doğru sonucu verecektir.

1. INTRODUCTION

Synthetic Aperture Radar (SAR) is a type of imaging radar, which uses signal-processing techniques to obtain finer resolution. The concept of the SAR was first described by Carl Wiley at Goodyear Company in 1951[1]. By the 1960s, the radar imaging would be so attractive because of its wavelength characteristic. They are active system (has own illumination), so they works well in darkness too. Radar frequencies pass through the clouds, rain and haze. Furthermore, radar waves scatter off materials differently that provides better discrimination for earth surface than optical sensor. Therefore, SAR has very wide range of application. These are topography changes, terrain mapping, sea and ice monitoring, oceanography, snow monitoring, mining etc. [2].

In most of the radar systems, platform moves along the direction of track with a constant velocity. The radar resolution is defined as along track (azimuth) resolution and across track (range) resolution. The pulse length determines across track resolution and it can be adjusted by transmitted signal. Along track resolution is determined by the beam width. In order to obtain a narrow beam width, the antenna length must be very long. It is not suitable to place a long antenna on the platform. In SAR system, a very long antenna is synthesized by the sensor motion and the signal processing techniques [3].

SAR uses different modes for collecting data from the ground. Strip map SAR, scanSAR, spotlight SAR and inverse SAR are some of these modes. In Strip map mode, pointing direction of the antenna does not change, indeed, it is kept constant, while the platform is moving. It images to a strip from ground and length of the strip depends on radar movement.

ScanSAR mode works similar with the strip map mode. In this system, antenna look angle is changeable so it scans different swaths. In this mode, azimuth resolution is worse than the strip map mode.

Different than the strip map SAR and scanSAR, spotlight SAR illuminates the ground by the beam which steers the interested area while the sensor is moving cross the scene. In inverse SAR, platform is stationary and target is moving or the platform also can be moving as well as the target [4].

SAR systems are based on sensor movement. In Figure 1.1, SAR geometry is given [4]. As shown in the figure radar moves along the azimuth axis. When radar is at the point P_2 beam centerline crosses the target. R denotes the slant range that is the distance between radar and target. Zero Doppler plane is the plane perpendicular to the sensor path, which includes the sensor. One of the important parameter about SAR geometry is squint angle (θ_{sq}). It is the angle between slant range vector and zero Doppler plane.

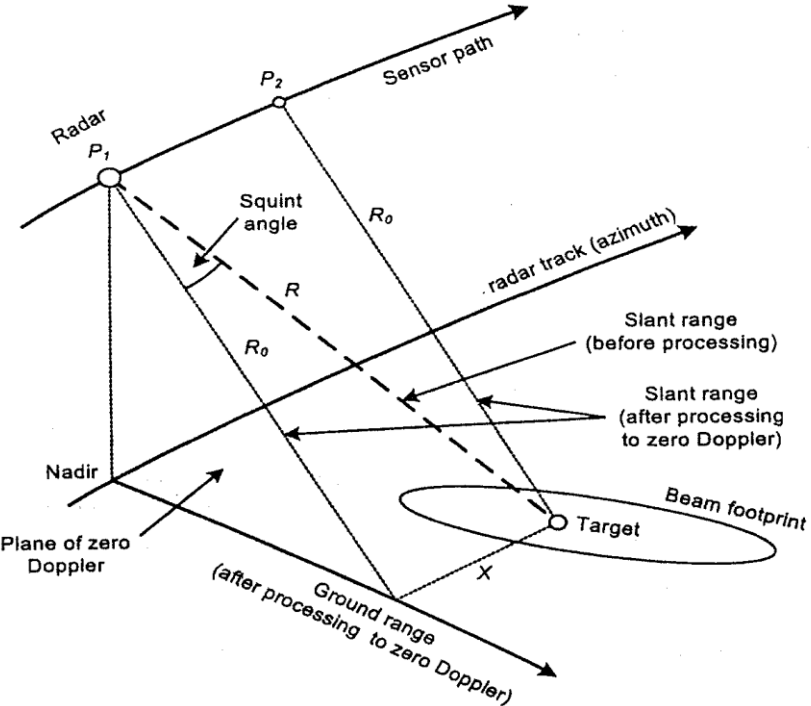


Figure 1.1 : SAR geometry.

In real aperture radar (conventional radars), a frequency modulated (FM) pulse is transmitted by the antenna. The pulse hits to the target and returns to the antenna. The time when the echo reach to the antenna, gives to the slant range. The smaller pulse length provides better range resolution. However, if the pulse length is too small, in this time signal to noise ratio (SNR) is reduced and the power that is needed for the transmission would be not enough. For this reason, FM signal is used for transmitted signal. This situation is the same for SAR. The difference occurs for the

azimuth resolution. Azimuth resolution is related to the beam width. The narrow beams gives better discrimination onto the ground. In SAR concept, in order to obtain narrow beam, long antenna is synthesized as shown in Figure 1.2 [4].

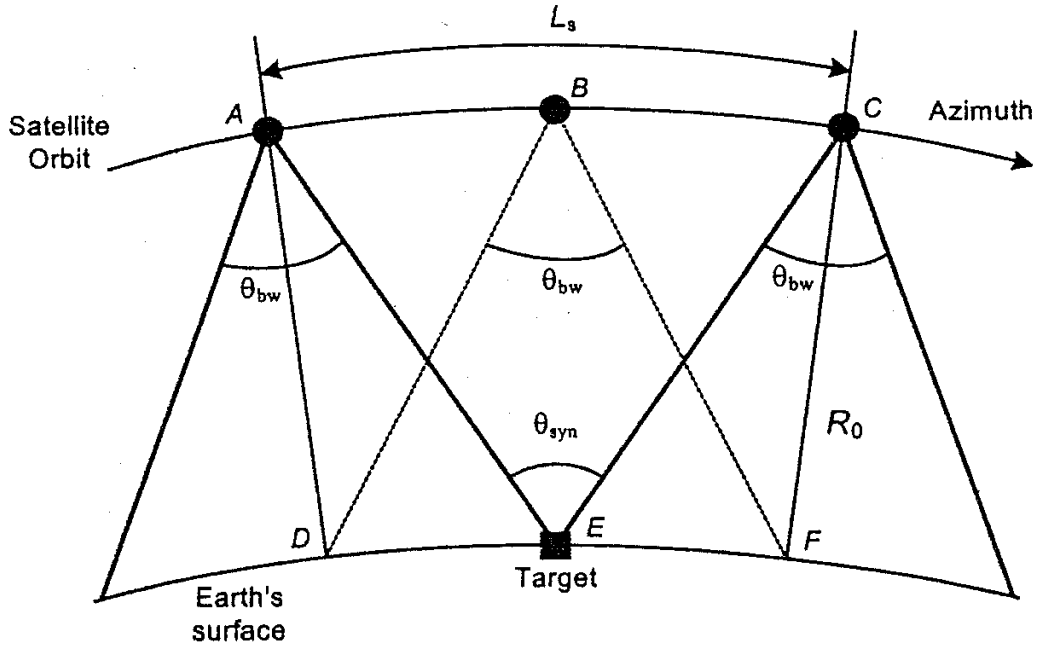


Figure 1.2 : Antenna beamwidth and synthetic aperture.

In the above figure, the radar acquires the first data for the target when the sensor position is at point A. The last data from the target is acquired when the sensor is at point C. The received data is recorded. θ_{bw} is the beam width in the azimuth direction. It is defined as $0.886 \lambda/L_a$, where L_a is the antenna length and λ is wavelength. θ_{syn} and L_s are the synthesized beam width and antenna length respectively. In order to synthesize a finer beam width and obtained high-resolution image in SAR system, signal-processing algorithms are used. Most common algorithm is Range Doppler Algorithm (RDA), which is used to obtain an image [4]. It is based on pulse compression techniques. The compression process is done for range and azimuth domain separately. For this processes, different matched filters with different frequency characteristics are used.

In fact, defining a matched filter in range domain is simple, because the filter parameter can be derived from the transmitted signal. However, for azimuth domain matched filter, the parameters cannot be derived easily. The received signal is shifted

because of sensor motion. This situation is called Doppler shift. Doppler centroid frequency must be known in order to find the amount of the shift.

1.1 Purpose of Thesis

In this thesis, Doppler centroid frequency is comprehensively analyzed for SAR systems. The importance of the Doppler centroid for the imaging algorithm is indicated. Different Doppler centroid estimation methods, which exist in the literature, are explained. In addition, effects of the incorrect Doppler centroid frequency on the image are presented.

The main purpose of the study is to present a new approach to minimize the effects of the incorrect Doppler centroid estimation. Proposed method is based on the block processing. Compared to the conventional methods, it is shown that the presented method here is more advantageous. The advantages of our approach is also presented.

1.2 Literature Review

In this part, first, SAR concept and Doppler centroid frequency is examined for background information. Then, RDA is presented as the imaging algorithm. After that, conventional methods in the literature, which are used to estimate the Doppler centroid, are given.

1.2.1 SAR resolution

Resolution in SAR system is defined as the capability of the system to distinguish between two points on the ground. Range resolution is depend on transmitted signal bandwidth and it is same real aperture radar. Range resolution is given in following equation [5].

$$\delta_r = \frac{c}{2B} \quad (1.1)$$

In this equation, c is the speed of light and B is the bandwidth of the transmitted signal. Bandwidth and pulse duration is inversely proportional. In order to obtain finer range resolution, the pulse duration should be lower.

Azimuth resolution is given in below.

$$\delta_a = \frac{\lambda R}{2L_s} = \frac{\lambda R}{2\left(\frac{\lambda R}{L}\right)} = \frac{L}{2} \quad (1.2)$$

λ is radar wavelength, R is the slant range, L_s is the synthesized antenna length and L is the real antenna length. The equation shows that, in SAR system antenna length should be smaller to obtain fine azimuth resolution.

1.2.2 SAR signal properties

In SAR system, the echo return from the target is recorded as a two dimensional matrix. The row of the matrix shows the range samples and the column of the matrix shows the azimuth samples. Actually received radar signal is one dimensional voltage value which is a function of time. It is recorded to a tape as shown in the Figure 1.3 [4]. The SAR antenna is used as both transmitter and receiver. After a linear FM pulse is sent, the receiver window is open and the returned signal is recorded. The returned signal is sampled. These samples is called as range samples. When the sensor moves, the other pulse is sent. The interval between two pulses is defined as pulse repetition interval (PRI). The frequency is called as pulse repetition frequency (PRF = 1/PRI). The azimuth signal is sampled with PRF. The azimuth samples varies with sensor position.

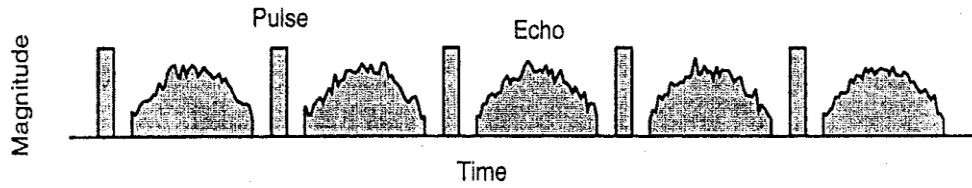


Figure 1.3 : Transmit and receive cycles.

The processing of raw data is done range and azimuth saperately. Therefore, the signals are considered two dimensional, range signal and azimuth signal respectively. In range dimension, radar transmits linear FM pulse. It is shown in the Equation (1.3).

$$s(\tau) = \text{rect}\left(\frac{\tau}{T_r}\right) \cos\{2\pi f_0\tau + \pi K_r\tau^2\} \quad (1.3)$$

Rectangular function gives the pulse envelope of the signal. T_r is pulse duration, K_r is the FM rate and f_0 is center frequency, which is derived from $f_0 = c/\lambda$. After the transmitted signal hits a point target at a distance R_a away from the sensor, the returned signal is given in Equation (1.4).

$$s_r(\tau) = A_0 \text{rect}\left(\frac{\tau - 2R_a/c}{T_r}\right) \times \cos\{2\pi f_0(\tau - 2R_a/c) + \pi K_r(\tau - 2R_a/c)^2 + \psi\} \quad (1.4)$$

The received signal has the same waveform as transmitted signal. However, it is attenuated, time shifted and there is a phase change ψ because of scattering process. The received signal also has a frequency shift which is caused by the sensor motion. When the distance between radar and target is decreased, the frequency of the received signal is increased. This situation is called as Doppler effect. The frequency which is related to the relative speed of the sensor and target is called SAR Doppler frequency. This event is presented in the Figure 1.4 [4].

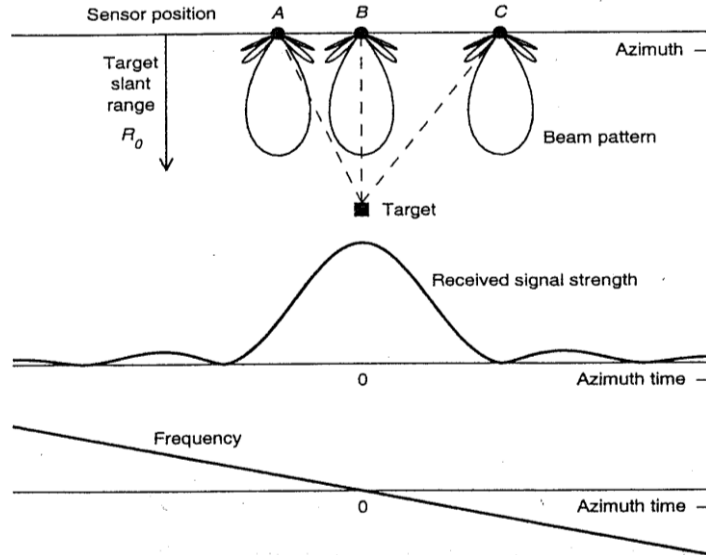


Figure 1.4 : Azimuth beam pattern and its effect on azimuth signal.

The sensor moves to the direction that indicated in the figure as azimuth. When the radar is at the position A, the radar starts to illuminate the target. The distance between target and sensor is minimum when the sensor is at the position B. The time is called beam center crossing time. The signal strength is decreases until the target

is not illuminated when the sensor passes the position C. The frequency change is shown at the bottom of the figure. This example is valid for one point target. If we mention about the ground imaging, we must consider the height of the earth surface. The received signal strength seems like a sincsquare function. When the azimuth time is η and beam center crossing time is η_c , the two dimensional received signal is defined as the following equation.

$$s(\tau, \eta) = Aw_r(\tau - 2R(n)/c)w_a(\eta - \eta_c) \times \cos \left\{ \begin{array}{l} 2\pi f_0(\tau - 2R(\eta)/c) \\ +\pi K_r(\tau - 2R(n)/c)^2 + \psi \end{array} \right\} \quad (1.6)$$

In the equation, w_r and w_a are the envelopes of the range signal and azimuth signal respectively. w_r is the rectangular function and w_a is the sinc-squared function.

The Figure 1.4 is handled again, the peak of the received signal is at the azimuth time is zero where the sensor is at the position B. The peak of the azimuth signal strength is called as Doppler centroid frequency. In this example, the sensor is supposed as not squinted. If the radar looks with an angle, the Doppler centroid frequency will not be zero. The Doppler band shifts with the squint angle [4].

1.2.3 Azimuth aliasing

In SAR system, the received signal is recorded after a demodulation process is done. That means that, the received signal is at baseband. In order to sample to the signal in range direction is not a problem because sampling frequency is determined by Nyquist criteria [6]. However, in azimuth direction, the sampling frequency is limited by PRF. The azimuth signal is not bandlimited, because the azimuth beam pattern is continued beyond the main lobe. The choice of the PRF is determined by the range swath. Therefore, azimuth signal sampling process cannot be appropriate to the Nyquist sampling rate. This causes to alias the signal in azimuth direction. It is an undesirable situation for the Doppler centroid estimation. Figure 1.5 presents an aliased azimuth signal [4]. In this example, the antenna pattern is not shown. The first row of the figure illustrates an unaliased signal, which is sampled with an high frequency rate (Nyquist rate). In the second row of the figure, the same signal is sampled by quarter of the Nyquist rate and aliasing has occurred. The last row of the figure shows the instantaneous frequency of the signal. The dashed line gives the

frequency of the unaliased signal and the solid line gives the frequency of the aliased signal. It is clear that the aliased signal repeat itself four times.

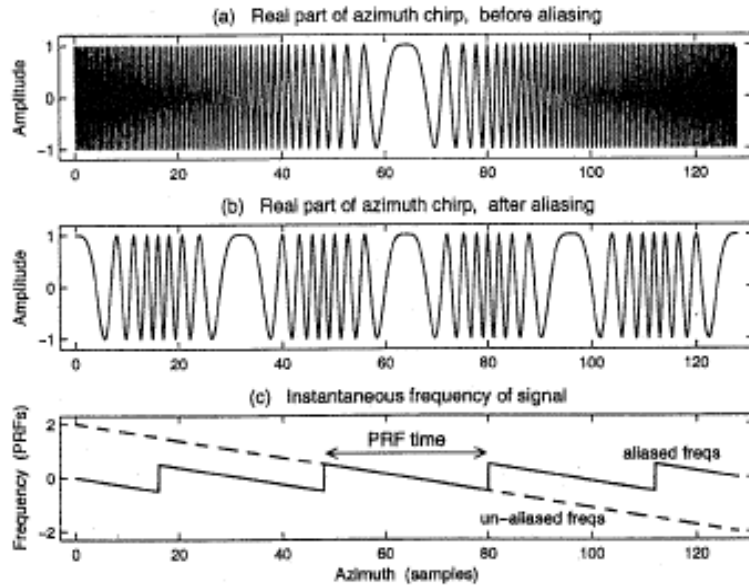


Figure 1.5 : Presentation of the azimuth aliasing caused by PRF sampling.

1.2.4 Doppler centroid

When the beam centerline crossing the target, azimuth signal gives maximum gain. This peak value is defined as Doppler centroid. Doppler centroid frequency is related to squint angle [4]. If the squint angle is zero, Doppler centroid would be zero, too. When the beam is squinted forward, Doppler centroid is positive. Because of the azimuth aliasing, Doppler centroid is not unique. There is an ambiguity about where the true center frequency is. In order to overcome this problem, it is considered as Doppler centroid consists of two parts, fractional part and integer part. It is derived from the equation.

$$f_{\eta_c} = f'_{\eta_c} + M_{amb}F_a \quad (1.7)$$

In the Equation (1.7) f_{η_c} is the absolute Doppler centroid, f'_{η_c} is the fractional part –it is also called as baseband part. M_{amb} is the ambiguity number, another definition of it is Doppler ambiguity and F_a is the PRF.

The baseband part of the Doppler centroid is enough for the azimuth domain matched filter. However, it is needed to know absolute part for the range cell migration correction, which is mentioned in the next section.

1.2.5 Range cell migration

Instantaneous slant range depends on the azimuth time. The range to the target $R(\eta)$ is given by the hyperbolic equation,

$$R^2(\eta) = R_0^2 + V_r^2 \eta^2 \quad (1.8)$$

where R_0 is the slant range when the radar is closest to the target, V_r is the sensor velocity. The equation presents the target trajectory, in range units. In signal memory, the trajectory migrates through range cells during the exposure time of the target, and it is called as range cell migration (RCM) [4].

This migration is important for SAR principle and essential parameter. However, it makes the processing complicated. The range cell migration should be corrected to simplify the processing.

1.3 Range Doppler algorithm

In SAR system, the most commonly used imaging algorithm is Range Doppler Algorithm (RDA). It was developed in 1976-1978 for processing SEASAT SAR data. The algorithm works efficiently especially block processing methods. The Fourier transformation is taken as one-dimensional, separately in range and azimuth domains. Therefore, it provides processing simplicity and efficiency [4]. In Figure 1.6, a basic RDA block diagram is presented. In this algorithm, range compression and azimuth compression process is done at different times. First, one dimensional Fast Fourier transform (FFT) is taken on the range samples and a frequency domain matched filter is created and is multiplied with frequency domain range samples for range compression. The range-compressed data is obtained by taking the inverse FFT of the filtered data. After that, one-dimensional FFT of the azimuth samples of the range compressed data is evaluated which means the data is at the Range Doppler domain. The Doppler centroid is estimated in this step. Range cell migration correction (RCMC) step is neglected in this study.

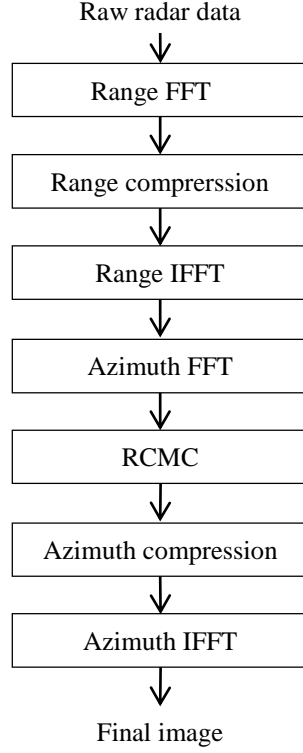


Figure 1.6 : RDA algorithm overview.

In RDA, the most important thing is the design of matched filters. The bandwidth and location of the filter should be defined to overlap the received signal. To remind SAR received signal properties, in Equation (1.9) gives the phase of the signal, envelopes are neglected [4].

$$s_0(\tau, \eta) = \exp\{-j4\pi f_0 R(\eta)/c\} \exp\{j\pi K_r(\tau - 2R(\eta)/c)^2\} \quad (1.9)$$

The Fourier transform of the signal $s_0(\tau, \eta)$ with respect to τ is given in the equation.

$$S_0(f_r, \eta) = \exp\left\{-j \frac{4\pi(f_0 + f_r)R(\eta)}{c}\right\} \exp\left\{-j \frac{\pi f_r^2}{K_r}\right\} \quad (1.10)$$

The second exponential term is quadratic phase term and it must be canceled. In order to do this, a frequency domain matched filter is designed as shown in the Equation (1.11). The matched filter must be complex conjugate of the quadratic phase term [4].

$$H(f_r) = \exp\left\{j \frac{\pi f_r^2}{K_r}\right\} \quad (1.11)$$

To finish the range compression process, the frequency domain signal and filter are multiplied and inverse FFT is taken. The range compressed signal expressed as the following equation.

$$s_{rc}(\tau, \eta) = IFFT_{\tau}\{S_0(f_r, \eta)H(f_r)\} = \exp\{-j4\pi f_0 R(\eta)/c\} \quad (1.12)$$

The range equation is substituted in the Equation (1.8). In low squint case, the range equation can be considered as parabolic form. Normally, it is in hyperbolic form. The range equation is given below.

$$R(\eta) = \sqrt{R_0^2 + V_r^2 \eta^2} \approx R_0 + \frac{V_r^2 \eta^2}{R_0} \quad (1.13)$$

In this equation, R_0 is distance between sensor and target according to closest approach, V_r is the sensor velocity and range compressed signal becomes following.

$$s_{rc}(\tau, \eta) = \exp\left\{-j\frac{4\pi f_0 R_0}{c}\right\} \exp\left\{-j\pi \frac{2V_r^2}{\lambda R_0} \eta^2\right\} \quad (1.14)$$

In the second exponential term, since the phase is a function of η^2 , the range compressed signal has linear FM characteristic and the FM rate is defined as $K_a = 2V_r^2/\lambda R_0$.

Then, azimuth FFT is taken on each range gate to transform the data range Doppler domain. The relationship between azimuth time and frequency, $f_{\eta} = -K_a \eta$. The data after azimuth FFT becomes following equation.

$$S_a(\tau, f_{\eta}) = \exp\left\{-j\frac{4\pi f_0 R_0}{c}\right\} \exp\left\{j\pi \frac{f_{\eta}^2}{K_a}\right\} \quad (1.15)$$

The first exponential term in the equation is constant for a given target and it is used for polarimetry and interferometry, second exponential term is important for intensity image, it gives the azimuth modulation. To complete azimuth compression azimuth matched filter is created as below equation [4].

$$H_a(f_{\eta}) = \exp\left\{-j\pi \frac{f_{\eta}^2}{K_a}\right\} \quad (1.16)$$

To define a proper matched filter azimuth frequency values must be known. The azimuth signal is shifted because of Doppler effect. The Doppler centroid frequency is calculated or estimated in this step. RCMC step is neglected for this study. Finally, IFFT is performed to filtered data and two-dimensional image is obtained.

The RDA process is tested on simulation data. Three targets are simulated with no squint. Two of the targets are at the same range line and two of them are at the same azimuth line. The data has 309 samples in range direction and 256 samples in azimuth direction. Their values are recorded in double. In the Figure 1.7, raw simulated data is shown.

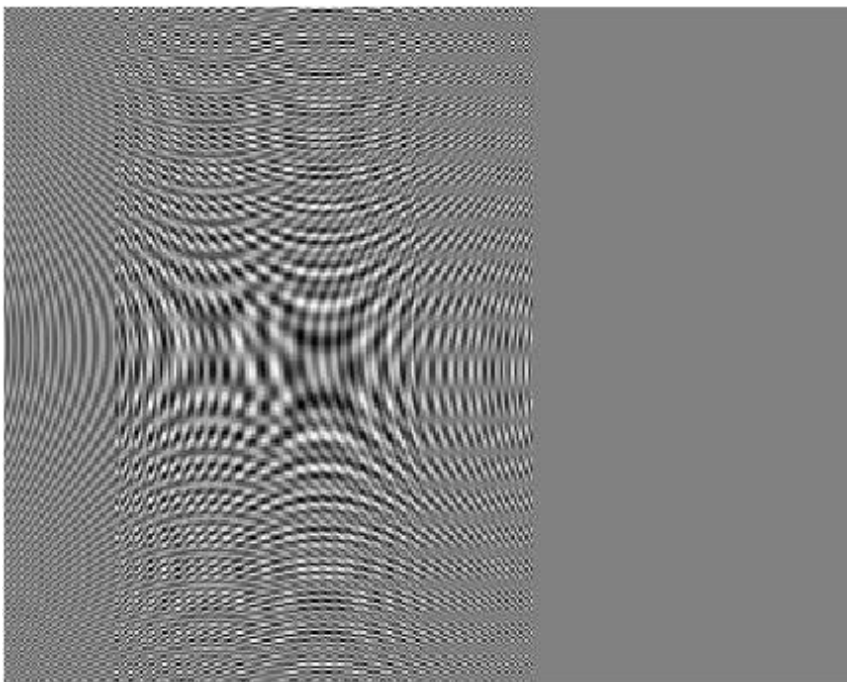


Figure 1.7 : Simulation of raw data with no squint case.

After a range FFT performed, the frequency domain data is multiplied by range matched filter. Then inverse FFT process is done and range compressed data is obtained. The Figure 1.8 shows the range compressed data obtained. data In the figure, two trajectories exist because two targets at the same range and they have the same trajectory. Then, an azimuth domain FFT is performed on range compressed data. Doppler centroid estimation is done after this step. In simulation, Doppler centroid is calculated from geometry. Doppler centroid is also zero, because the squint angle is zero. Frequency domain data is multiplied by azimuth domain matched filter and inverse FFT is taken.

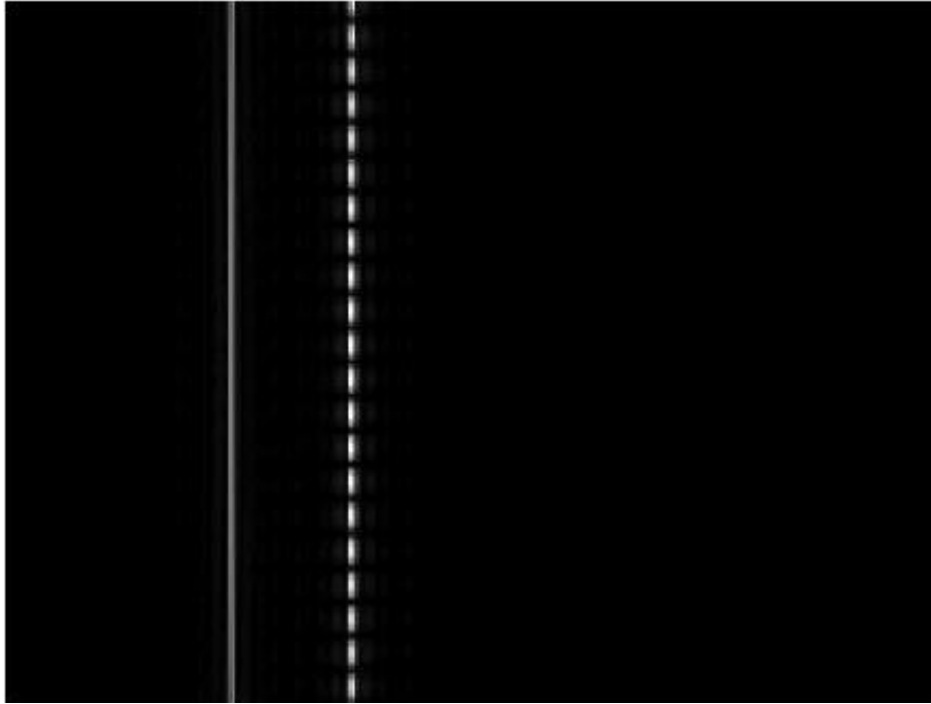


Figure 1.8 : Range compressed data (no squint case).

The resultant data is the final image. It is shown in Figure 1.9.

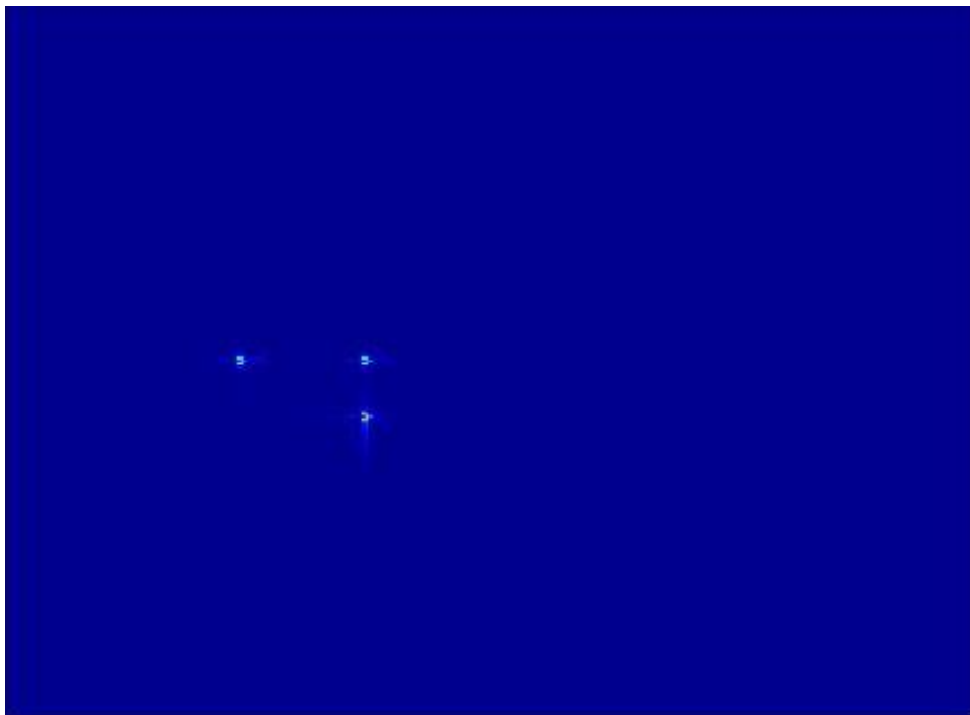


Figure 1.9 : Final image after azimuth compression (no squint case).

The previous example is in the case that the squint angle is zero. When the squint angle exists and its value is high, the processing would be complicated. Doppler

centroid calculation should be done effectively. The Figure 1.10 simulates the raw data with a 10° squint angle. Range compressed data is shown in Figure 1.11.

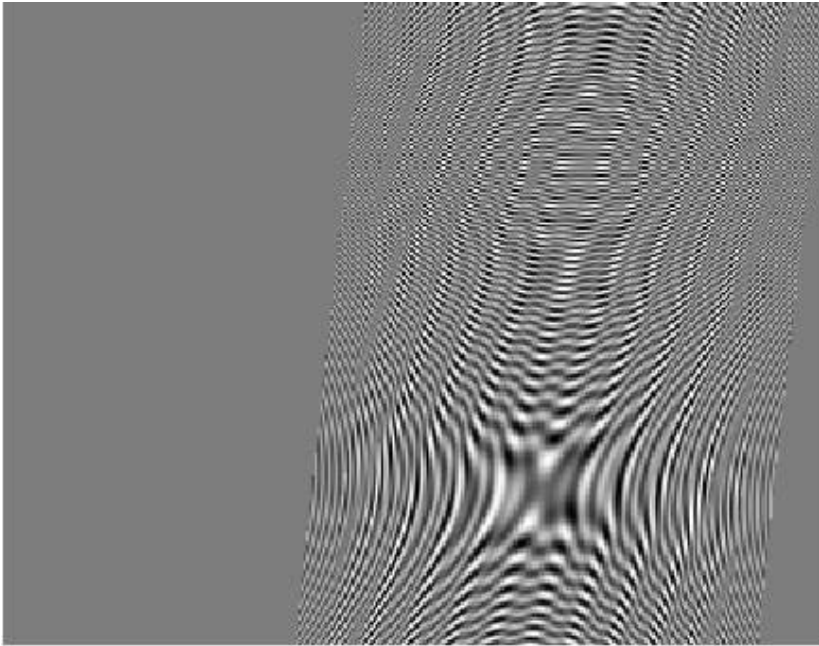


Figure 1.10 : Simulation of raw data which has a 10° squint angle.

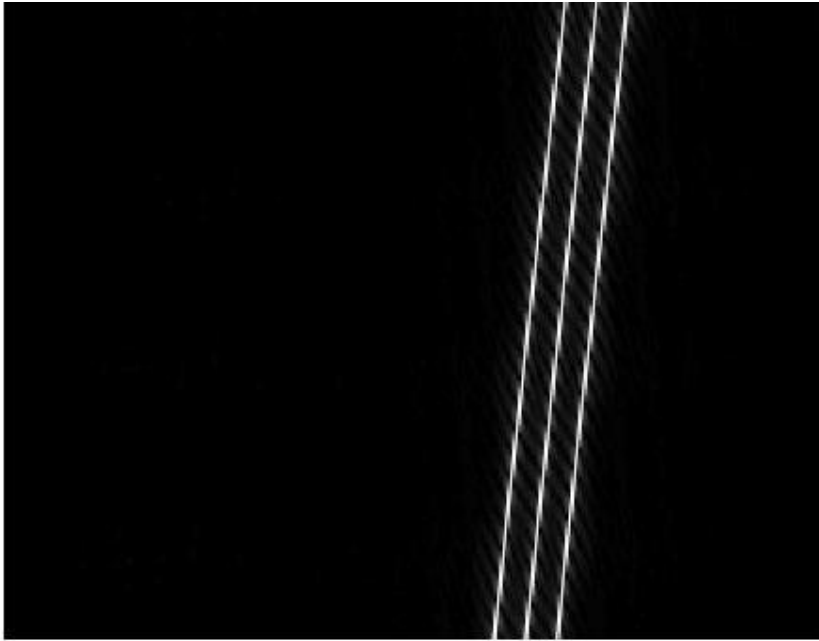


Figure 1.11 : Range compressed data (squinted case).

The effects of the squint angle obviously appear in the figures. In this example, the three targets lie at the same azimuth line. The Doppler centroid is calculated azimuth compression process is done with Doppler centroid and without Doppler centroid. In

Figure 1.12, the final image with a -90 Hz Doppler centroid is presented. The Figure 1.13 presents the final image which is processed with zero Doppler centroid.

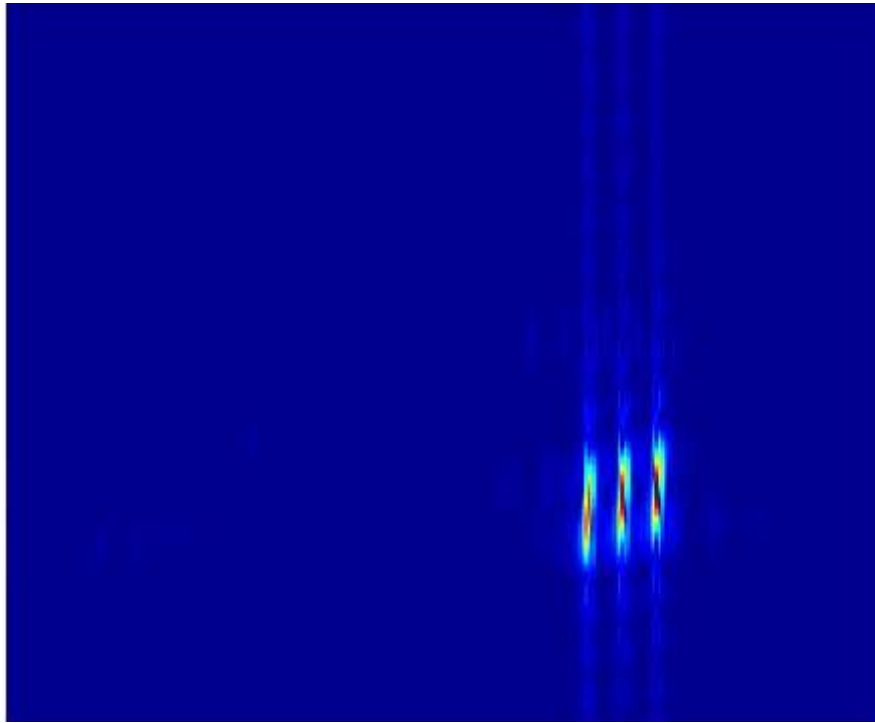


Figure 1.12 : Final image that processed with a -90 Hz Doppler centroid.

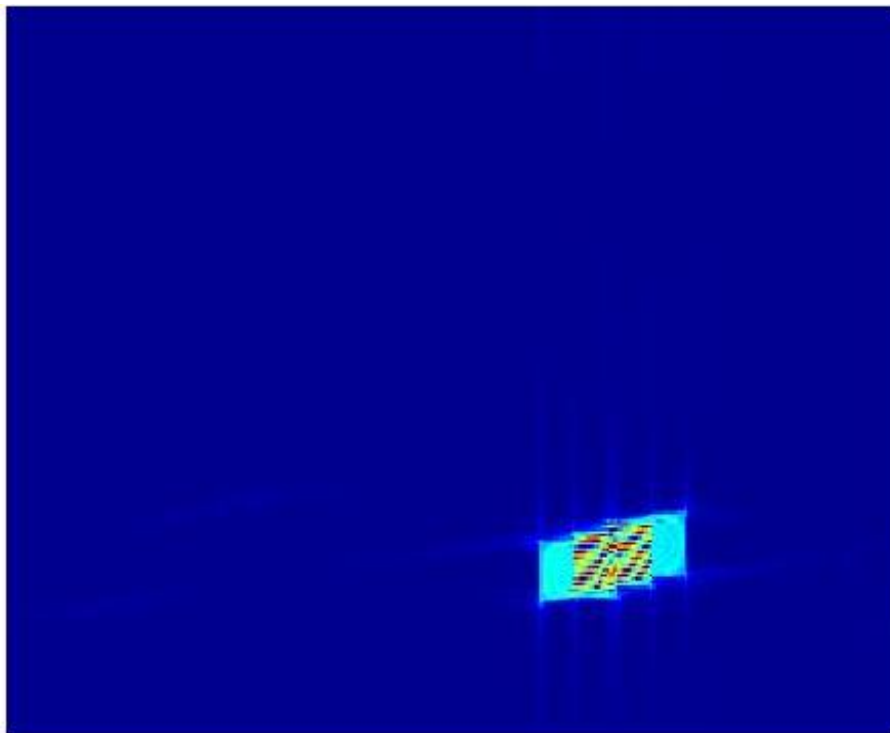


Figure 1.13 : Final image that processed with zero Doppler centroid.

As shown in the figure, if the Doppler centroid is not estimated correctly, there will be the distortions in the final image. The results shows that, the Doppler centroid is an important parameter for SAR processing and it should be estimated correctly and efficiently.

1.4 Doppler Centroid Estimation

Doppler centroid can be calculated from the SAR geometry [4]. In satellite SAR, orbit and attitude information is necessary. However, accurate orbit geometry information cannot be always provided. In airborne SAR, the undesired aircraft motions usually caused by weather condition do not allow to obtain accurate geometric information. Furthermore, scene contents such as landforms, buildings etc. also affect the geometry calculations. Estimating Doppler centroid from the received data is a well-known technique. There are a lot of studies in the literature on this topic [7-13]. Doppler centroid is composed of two parts according to their usage: the fractional part and the integer part. The estimation process is done for the two parts separately. In this section, firstly the calculation process from the SAR geometry is explained. After that, baseband Doppler centroid estimation methods and Doppler ambiguity resolver methods, which is used to define estimation of the absolute Doppler centroid, is presented respectively.

1.4.1 Doppler centroid calculation from geometry

In this section, it is explained how Doppler centroid is calculated by using a geometry model. To calculate the centroid, orbit attitude and pointing direction of the radar beam must be known. The computed Doppler centroid is absolute Doppler centroid. In this calculation, relative velocity between radar and a beam-center target on the Earth surface must be computed. Doppler centroid frequency is then calculated by,

$$f_{\eta_c} = -\frac{2V_{rel}}{\lambda} \quad (1.17)$$

For an aircraft case, Doppler centroid calculation is done as following,

$$f_{\eta_c} = \frac{2V_r \sin \theta_{r,c}}{\lambda} \quad (1.18)$$

where the V_r is the aircraft velocity and $\theta_{r,c}$ is squint angle. In the satellite case, the calculation is more complicated because of the Earth curvature [4].

To obtain the necessary information for this calculation is not easy. Especially, in the airborne case, the sensor attitude and velocity is not stable. Therefore, Doppler centroid estimation from the received data is well known techniques in the literature.

1.5 Baseband Doppler Centroid Estimation

The baseband Doppler centroid, which is used to design a proper azimuth matched filter, is estimated by using two approach. These are magnitude based estimation approach and phase based estimation approach. In the literature, a number of algorithms exist which are used these approaches. The approaches are examined separately in the next section.

1.5.1 Magnitude based Doppler centroid estimation approach

In this approach, the power spectrum of the azimuth signal gives an estimate of the baseband Doppler centroid. Power spectrum of the azimuth signal appears to antenna beam pattern and when the beam center crosses the target, a peak occurs at that frequency. The frequency where the peak value occurs, is the Doppler centroid frequency. In this method, power spectrum of the azimuth signal is calculated for every range bin. The spectrums are affected from the noise and ground reflectivity. To prevent this effects, the spectrums of the whole range bin are summed and averaged. The shape of the averaged spectrum looks like a Gaussian curve. The peak of the curve gives the Doppler centroid [4]. Figure 1.14 presents this situation. In the first row of the figure, the power spectrum of one range bin is shown. It is too noisy and meaningless. The averaged spectrum is presented in the second row of the figure. The shape of the spectrum resembles to the antenna beam pattern, but it is still noisy and actual peak of the spectrum cannot be found. The noise of the spectrum are high frequency components. When a low pass filter is applied to the averaged spectrum, the bottom image is obtained. Finally the Doppler centroid frequency is taken as the frequency where the power has the maximum value as illustrated with the dashed-red line in the same figure.

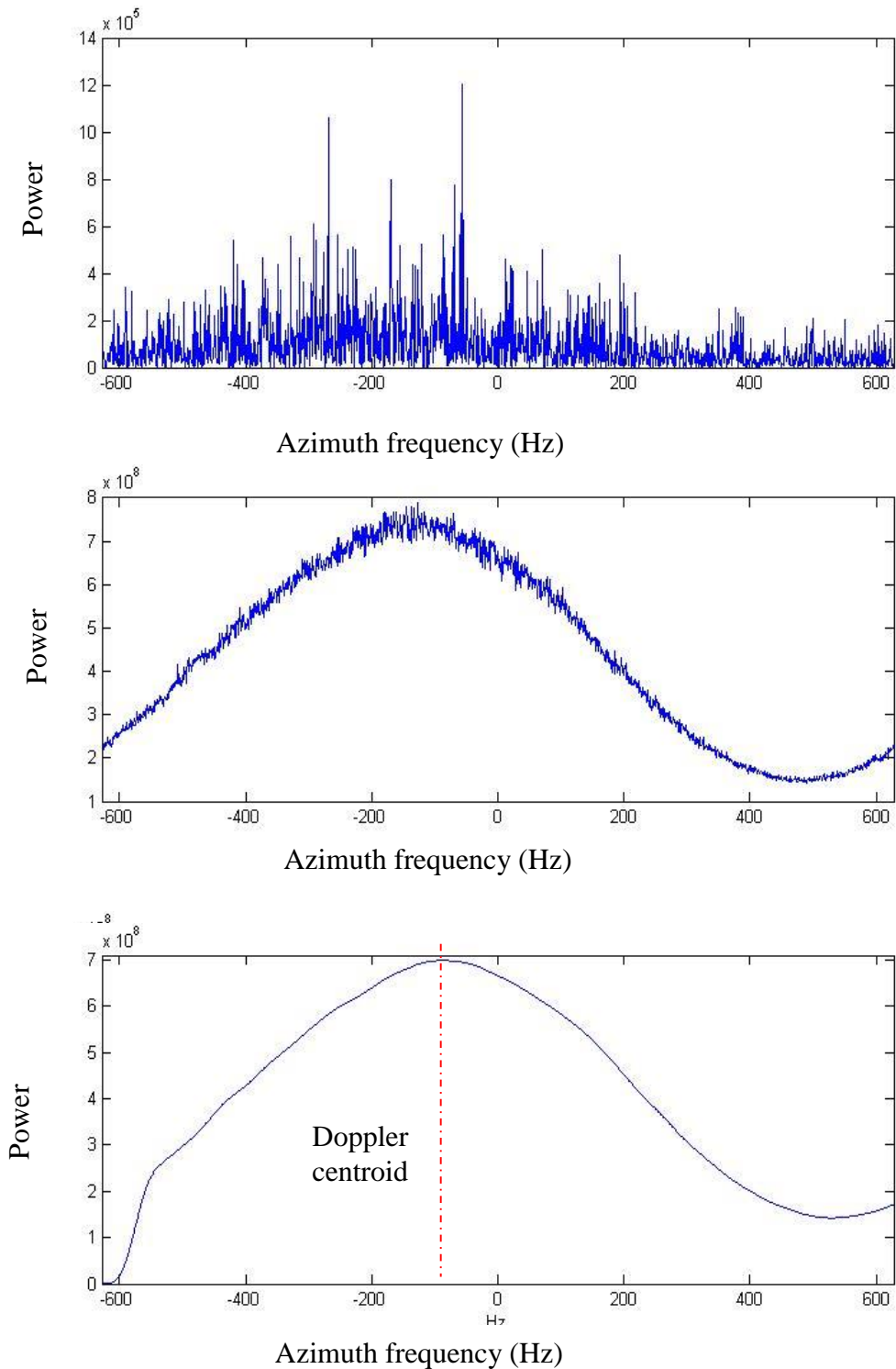


Figure 1.14 : Magnitude based Doppler centroid estimation approach.

In the literature, there are number of algorithms that uses the magnitude based approach [9]. Some of the algorithms work on azimuth signal of the raw data, some of them work on the azimuth signal of the range-compressed data. Furthermore, some processors uses power balancing filter instead of low pass filter.

1.5.2 Phase-based Doppler centroid estimation approach

This approach is introduced by Madsen in 1989. This approach may be called as phase increment method [7]. The phase of the complex SAR data can be used to find baseband Doppler centroid. The difference of the signal phase between azimuth samples constitute the principle of the method.

Let $s(\eta)$ be a sample of the azimuth signal, and $s(\eta + \Delta\eta)$ be the next sample. $\Delta\eta$ is the azimuth time interval which is equal to $1/PRF$. The signal difference can be found as following.

$$\Delta s(\eta) = s^*(\eta)s(\eta + \Delta\eta) \quad (1.19)$$

The signal difference vectors are summed and averaged to prevent the phase unwrapping problem. The average phase increment is given in the Equation (1.20).

$$\overline{C(\eta)} = \sum_{\eta} s^*(\eta)s(\eta + \Delta\eta) \quad (1.20)$$

When the angle is only concerned, the averaging process is done using sum operation. s^* denotes complex conjugate of the signal s . $\overline{C(\eta)}$ is called average cross correlation coefficient (ACCC). The expected value of the angle of the ACCC is given in the following equation.

$$\phi_{acc} = \text{angle}(\overline{C(\eta)}) \quad (1.21)$$

ACCC angle equals to phase increment, at the center of the exposure, $\eta = \eta_c$. Average phase increment is then,

$$\phi_{acc} = \left. \frac{d\phi(\eta)}{d\eta} \right|_{\eta=\eta_c} \Delta\eta = -\frac{4\pi f_0 V_r^2 \eta_c}{cR(\eta_c)} \Delta\eta = -\frac{2\pi}{F_a} K_{a,dop} \eta_c \quad (1.22)$$

where F_a is the PRF and $K_{a,dop}$ is the averaged azimuth FM rate. Then Doppler frequency is,

$$f_{\eta_c} = -K_{a,dop}\eta_c \quad (1.23)$$

Baseband Doppler centroid is given in the Equation (1.24).

$$f'_{\eta_c} = \frac{F_a}{2\pi} \Phi_{acc} \quad (1.24)$$

1.6 Doppler Ambiguity Resolver (DAR)

In the literature, there are lots of study for this topic. The most using algorithms are examined in two parts, as magnitude based and phase based algorithms in the following section.

1.6.1 Magnitudebased DAR estimation method

The goal of the DAR algorithms is estimate to true ambiguity number, M_{amb} . In this method, the correlation between two azimuth look gives an explanation about misregistration in the range direction. The misregistration between the two looks can be measured by correlating the magnitude images of each look in the range direction, and averaging on many range lines. The algorithm works well on the high contrast scene. If enough averaging is done, it can work on the low contrast scene.

1.6.2 Phasebased DAR estimation method

Absolute Doppler centroid is a linear function of radar carrier frequency, f_0 . The phased based DAR estimation method uses this principle. When the ACCC angle is plotted versus range frequency, in order to find absolute Doppler centroid, average slope of the values can be used. It also works on aliased spectrum. The value of the ambiguity number that makes the intercept closest to zero.

There are three methods to determined the variation of the Doppler centroid versus range frequency. These are wavelength diversity algorithm, multilook cross correlation algorithm and multilook beat frequency algorithm.

Wavelength diversity algorithm (WDA) is developed in German Aerospace Center, DLR [13]. In this algorithm, the slope of the ACCC angle versus range frequency is used to estimate range frequency dependence of the Doppler centroid. The steps of

the algorithm, first a FFT is performed on the range samples, then ACCC angle is calculated for every range frequency cell and signal increments in the azimuth direction is found. The angle of the average phase increment is calculated. The slope of the range frequency is found using regression. Then the ACCC angle can be written as below equation.

$$\Phi_{accc}(f_r) = -\frac{2\pi}{F_a} \frac{2V_r^2(f_0 + f_r)}{cR(\eta_c)} \eta_c \quad (1.25)$$

The slope of this equation is following.

$$\alpha = \frac{d\Phi_{accc}(f_r)}{df_r} = -\frac{2\pi}{F_a} \frac{2V_r^2}{cR(\eta_c)} \eta_c \quad (1.26)$$

Then substituting azimuth FM rate in this equation, the absolute Doppler centroid is derived as the Equation (1.27).

$$f(\eta_c) = \frac{F_a}{2\pi} f_0 \alpha \quad (1.27)$$

The other method is used to phase based DAR, multilook cross correlation (MLCC) algorithm [9]. In this method, two range looks are used to eliminate the effect of range frequency on the Doppler centroid. The ACCC angle of two looks are calculated. The difference between azimuth FM rate of the two looks, gives the difference between ACCC angle. Let ACCC angle of the two looks are,

$$\Phi_{L_1} = -\frac{2\pi}{F_a} K_{a1,dop} \eta_c \quad (1.28)$$

$$\Phi_{L_2} = -\frac{2\pi}{F_a} K_{a2,dop} \eta_c \quad (1.29)$$

where $K_{a1,dop}$ and $K_{a2,dop}$ are the averaged FM rate of the two looks evaluated as,

$$K_{a1,dop} = \frac{2V_r^2}{cR(\eta_c)} \left(f_0 - \frac{\Delta f_r}{2} \right) \quad (1.30)$$

$$K_{a2,dop} = \frac{2V_r^2}{cR(\eta_c)} \left(f_0 + \frac{\Delta f_r}{2} \right) \quad (1.31)$$

The difference between two look angle,

$$\Delta\phi = \phi_{L_2} - \phi_{L_1} = -\frac{2\pi}{F_a} (K_{a2,dop} - K_{a1,dop})\eta_c \quad (1.32)$$

$$\Delta\phi = \text{angle}\{[\overline{C_1(\eta)}]^* \overline{C_2(\eta)}\} \quad (1.33)$$

To avoid wraparound the phase are subtracted. The difference angle is written as,

$$\Delta\phi = -\frac{2\pi}{F_a} \frac{\Delta f_r}{f_0} K_{a,dop} \eta_c = -\frac{2\pi}{F_a} \frac{\Delta f_r}{f_0} f_{\eta_c} \quad (1.34)$$

$$f_{\eta_c} = \frac{F_a}{2\pi} \frac{f_0}{\Delta f_r} \Delta\phi \quad (1.35)$$

Multilook beat frequency (MLBF) algorithm is works as MLCC, but in this algorithm two looks are multiplied to find the Doppler frequency difference caused by range frequency shift. This algorithm beats (multiplies) two looks first.

$$s_{beat}(\eta) = s_1^*(\eta)s_2(\eta) = |w_a(\eta - \eta_c)|^2 \exp\left\{-j \frac{4\pi\Delta f_r R(\eta)}{c}\right\} \quad (1.36)$$

The beat signal is approximately a sine wave. If the frequency of the sine wave can be estimated, the absolute Doppler centroid can be found. The average beat frequency is,

$$f_{beat} = \frac{2\Delta f_r}{c} \frac{dR(\eta)}{d\eta} \Big|_{\eta=\eta_c} = -\frac{\Delta f_r}{f_0} f_{\eta_c} \quad (1.37)$$

and absolute Doppler centroid is calculated as following equation.

$$f_{\eta_c} = -\frac{f_0}{\Delta f_r} f_{beat} \quad (1.38)$$

The value of the beat frequency can be estimated by measuring the ACCC angle of the beat signal. Another way to estimate beat frequency is to find the peak in the magnitude spectrum of the beat signal.

If the DAR algorithms are compared, MLCC and WDA algorithms are similar in their operation and accuracy. MLBF algorithm works better the presence of bright targets. MLCC and WDA algorithms works well on the low contrast scene. On the contrary, in high contrast scene, the MLBF algorithm is preferred.

1.7 Hypothesis

In the literature, numbers of study exist for Doppler centroid estimation. The algorithms work well on real SAR data within different conditions. In this study, an alternative method is presented for Doppler centroid estimation. In the other methods, Doppler centroid is estimated for the whole scene. The fact that, Doppler centroid depends on the scene content. If the scene is formed of water, buildings, and mountainous area, the Doppler centroid will be averaged, and will be exact value for none of them. According to this study, the scene is divided to the sub-scene and the Doppler centroid is estimated for every sub-scenes, separately. In other words, the RDA is applied on the sub-scene, which is also defined as block, using their own Doppler centroid. This method is called block processing approach. In the next section, the result are examined for both conventional methods and block processing methods, too.

2. EXPERIMENTAL RESULTS

The algorithm is tested on the RADARSAT-1 raw signal data, which is given in [4]. The data were acquired on June 16, 2002 from the Vancouver, Canada. RADARSAT-1 data is recorded in CEOS format. It has some header information. In order to obtain the raw data, a MATLAB program exists in the CD, which name is "Read_Raw_SAR_CEOS". This program transforms the data to a matrix format by using the header data. RADARSAT-1 parameters are given in Table 2.1. After the data extracted, the RDA algorithm is rearranged using these parameters.

Table 2.1: RADARSAT-1 parameters.

Parameter	Symbol	Value	Units
Sampling rate	F_r	32.317	MHz
Range FM rate	K_r	0.72135	MHz/ μ s
Pulse duration	T_r	41.74	μ s
Radar frequency	f_0	5.3	GHz
PRF	F_a	1256.98	Hz
Azimuth FM rate	K_a	1733	Hz/s

In this program, the interested area can be selected. It is also possible to define the size of the matrix which belong to the interested area in the program. The area that covers the Vancouver Airport, is selected for the processing. The raw data is shown in the Figure 2.1. This area contains 2048 samples in the range domain and 1536 samples in the azimuth domain.

The data is transformed to frequency domain and a range domain matched filter is designed. The range domain matched filter is presented in the Figure 2.2. When we used the filter onto the data that is in frequency domain, ranged compressed data is obtained and it is shown in the Figure 2.3.

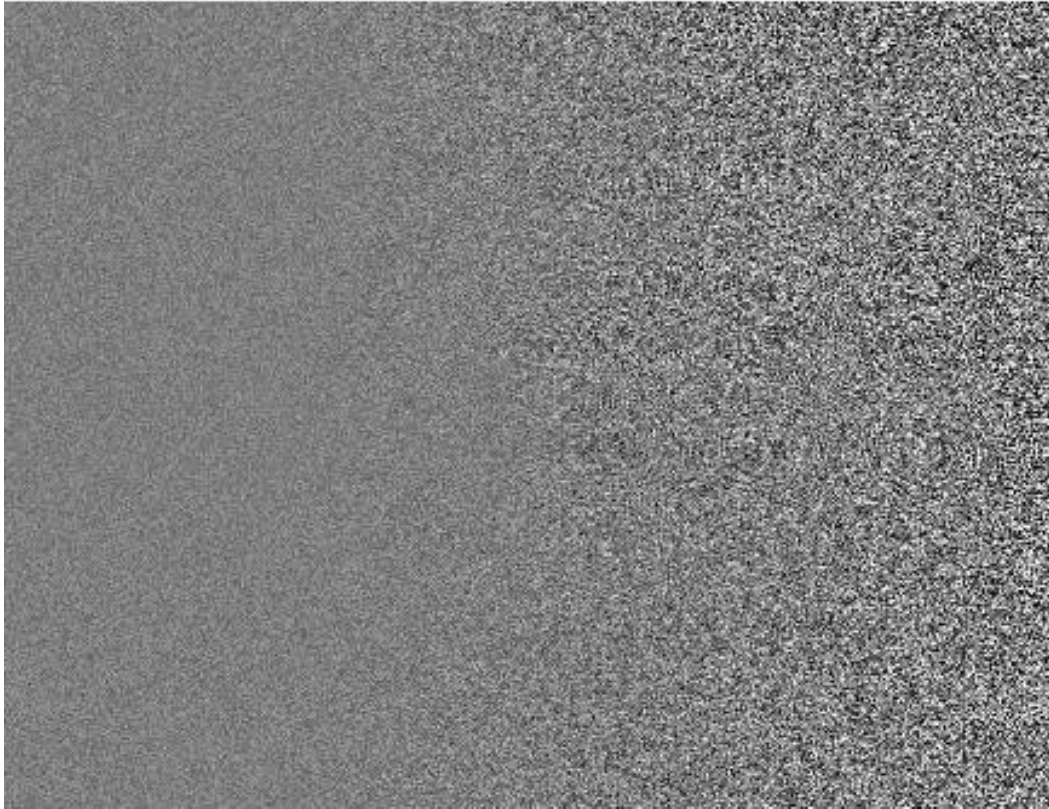


Figure 2.1 : Raw data of the Vancouver Airport.

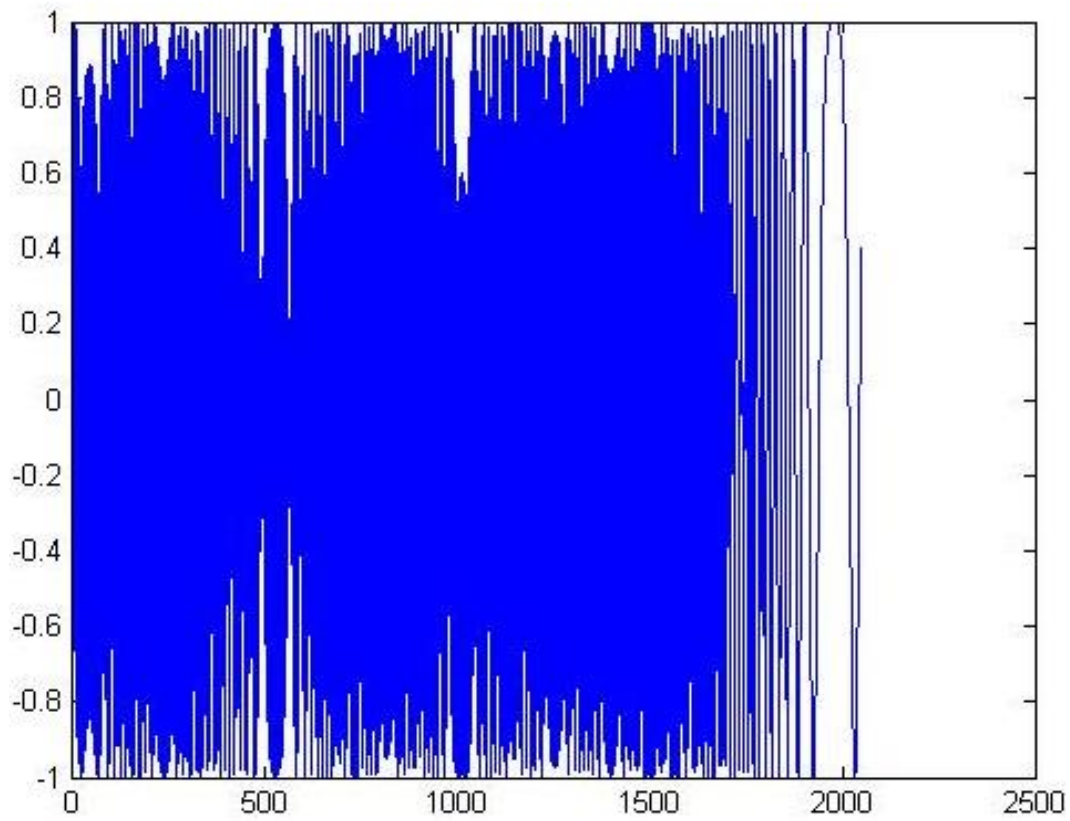


Figure 2.2 : Range domain matched filter.

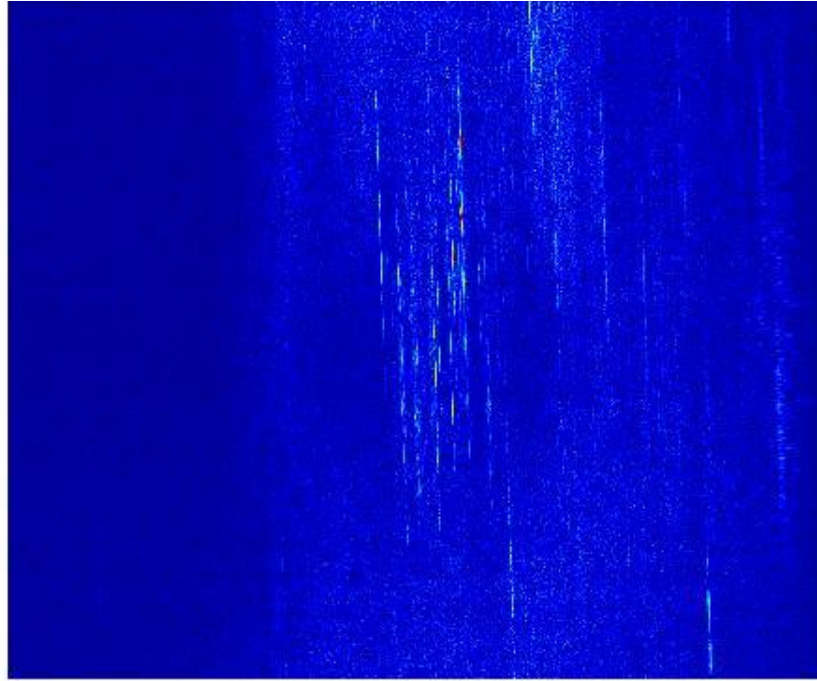


Figure 2.3 : Range compressed data.

After that, Doppler centroid is estimated and azimuth domain matched filter is designed. The magnitude-based approach is used for Doppler centroid estimation. In this study, RCMC step is neglected, so Doppler ambiguity estimation does not need to do. Only baseband part is estimated. Averaged power spectrum of the azimuth signal is filtered by a low pass filter. Filtered spectrum is presented in Figure 2.4.

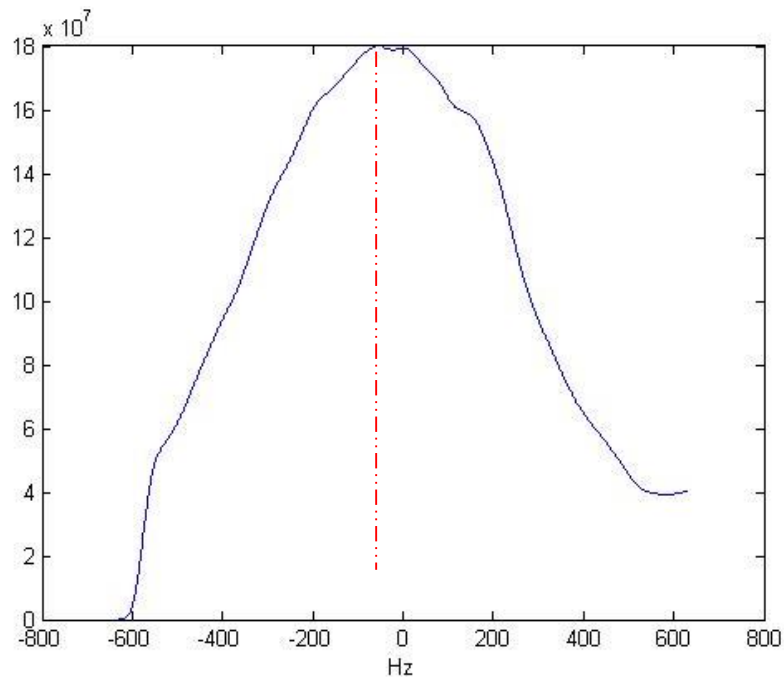


Figure 2.4 : Doppler centroid estimation result.

Doppler centroid frequency is taken as the frequency where the power has the maximum value as illustrated with the dashed-red line. The azimuth domain matched filter is designed using the estimated Doppler centroid value. After azimuth filtering an inverse FFT performed on azimuth compressed data and high resolution image is obtained. Azimuth domain matched filter and obtained image are shown in Figure 2.5 and Figure 2.6, respectively.

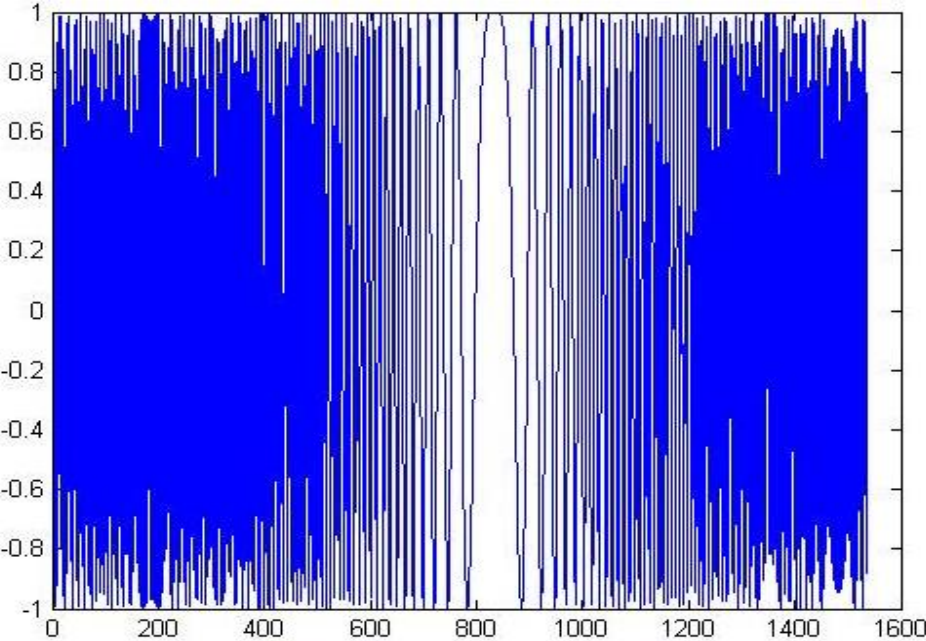


Figure 2.5 : Azimuth domain matched filter.



Figure 2.6 : Final image.

Next, there are some example that are processed in RDA. In the Figure 2.7, Stanley Park region is shown. The Doppler centroid of the data is estimated as -90 Hz.



Figure 2.7 : Stanley Park region.

Figure 2.8 presents Brackendale region. The data is processed with a Doppler centroid, -35 Hz.

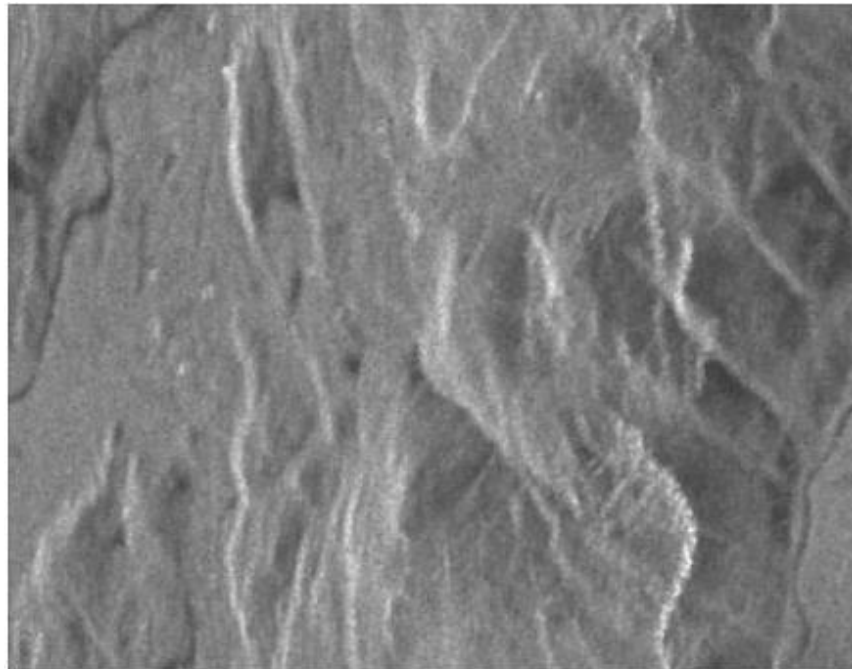


Figure 2.8 : Brackendale region.

In the Figure 2.9, the English Bay ships are seen. The Doppler centroid of the data is -95 Hz.



Figure 2.9 : The region of English Bay ships.

The resultant images are different regions of the Vancouver city. The image of the whole data is also obtained. The image has 9000 samples in range axis and 16000 samples in azimuth axis. The baseband Doppler centroid of the whole image is obtained -255 Hz in one PRF. Figure 2.10 presents the image that is obtained from the whole data.

The process takes too much computation time. When the concerning area is a small part of the scene, it is not wanted to wait for the whole process. Taking small parts of the scene is saved the processing time. To observe the accuracy improvement of the proposed method, the data is processed by dividing it into small parts and applying the azimuth filtering to each part of the data by obtaining their Doppler centroids independently.

It is realized from the results that some of ships are not seen in the full image, but they are seen in the sub-scene. The situation is presented in the Figure 2.11.

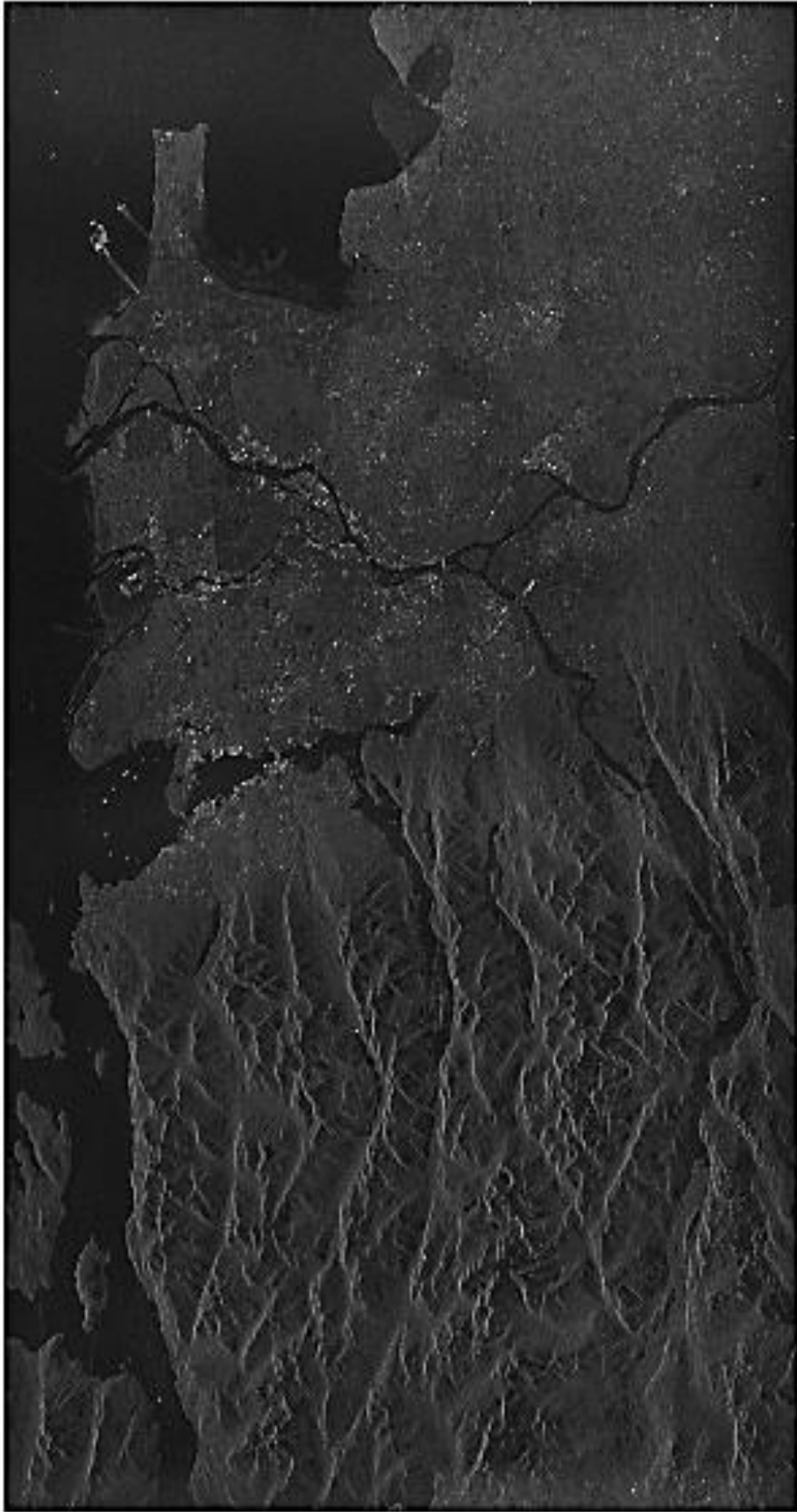


Figure 2.10 : Obtained image from whole data (Vancouver city).

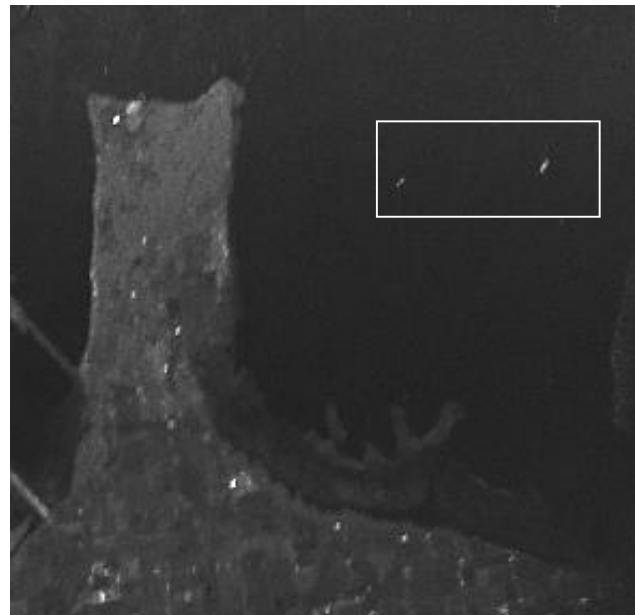


Figure 2.11 : Unseen targets.

The zoom of the image, which obtained from whole data is shown in the first row of the figure. The bottom of the figure presents the processed image after it divided sub-region. The ships are found away from the scene center therefore in the fully processed image they are not seen. When image is divided and the part that ships exist is processed with its own Doppler centroid, the ships have been appeared. This is also due to the different characteristics of the scene for different locations and average Doppler centroid obtained for the whole data could not reflects the scene characteristics of different regions.

Another improvement observed for the block processing is, some areas that are seen in the full image is not exactly in there. Figure 2.12 is an example for this situation.

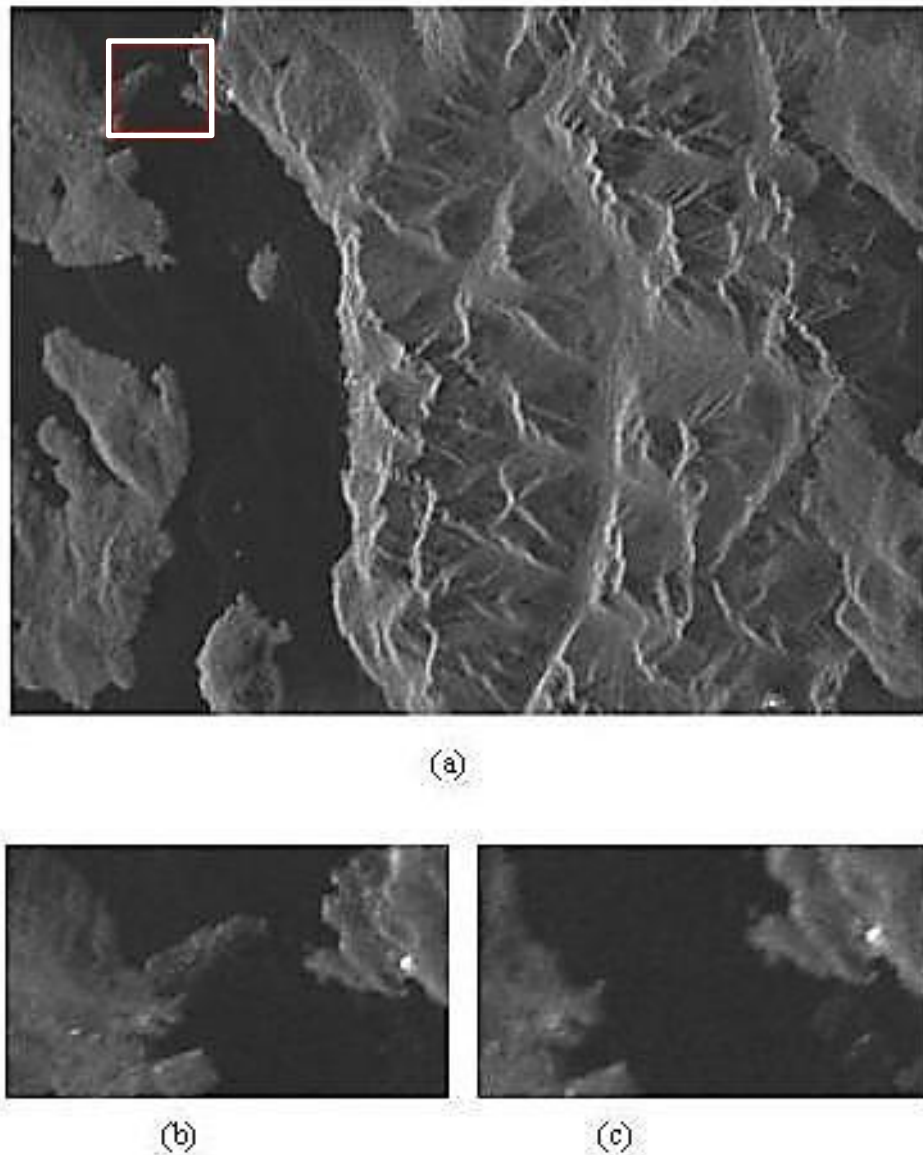


Figure 2.12 : Doppler centroid errors.

In the first row of the figure, in the red rectangle a part of land is shown. In reality, there is no such part of land at that section. It appears because of Doppler processing error. When we used block processing method, the image gets better and the land part is not seen in it. The (b) part of the figure zooms to the red rectangle. Block processing result is presented in the (c) part of the figure. It is clear from the figure, the elevation of the area varies. The height difference between the sea and mountain is so much. It affects the Doppler centroid calculations negatively. When we take an area whose elevations are nearly same, the Doppler centroid is estimated correctly.

3. CONCLUSIONS AND RECOMMENDATIONS

Doppler centroid is an important parameter for the SAR processing. If the Doppler centroid is not estimated correctly, there will be some distortions in the final image. In the RDA algorithm, baseband Doppler centroid is used for the azimuth compression process. The estimation of the baseband Doppler centroid is done using the magnitude-based approach.

In the thesis, an alternative method is presented for Doppler centroid estimation problems. Doppler centroid depends on some parameters. These are squint angle, scene content, motion of the platform etc. If the squint angle were high, the effects of the Doppler centroid estimation errors would be significant. The previous examples, the squint angle is not high, so the effects of the incorrect Doppler centroid could not be perceived. The other parameter is scene content that is really important for our approach. In the conventional methods, Doppler centroid estimation is done for the whole scene. The Doppler centroid is averaged and the results would be worse. In our approach, the data is divided to the sub-scene and every sub-scene is processed with their own Doppler centroids. The results of the new approach are satisfied. Some of the targets, which are not seen in the image that is processed with the conventional methods, become visible. If the squint angle were high, the much more effects would be observed. The motion of the platform does not affect the results. Because, motion compensation systems minimize that effects in satellite SAR. If the system were airborne SAR, the motion effect would be significant. The proposed method is also saving processing time.

In this approach, the selection of the sub-scene is important. The selected region should be have the elevation nearly same. The area of the mountain should constitute a sub-scene, the sea should constitute another sub-scene. The residential area is selected as a different sub-scene. If these areas are not divided into different region, the Doppler centroid will not be estimated correctly.

This method can be developed in the later studies. In order to increase the accuracy of this method, the RCMC algorithms can be applied before the azimuth compression. The segmentation of the sub-region could be done automatically.

REFERENCES

- [1] **Skolnik, M. I.**(2001).*Introduction to Radar Systems*.McGraw-Hill, New York.
- [2] **Curlander, J., McDonough, R.** (2005).*Synthetic Aperture Radar: System and Signal Processing*.John Wiley & Sons, New York.
- [3] **Massonnet, D., Souyris, J. C.** (2008).*Imaging with Synthetic Aperture Radar*.EPFL Press, Lausanne.
- [4] **Cumming, I. G., Wong, F. H.** (2005).*Digital Processing of Synthetic Aperture Radar Data: Algorithms and Implementations*.Norwood M.A., Arctech House, Inc.
- [5] **Chan, Y. K., Koo, V. C.** (2008).An Introduction to Synthetic Aperture Radar (SAR).Progress in Electromagnetics Research B, pp. 27-60.
- [6] **Oppenheim, A. V., Schaffer, R. W.** (1989) *Discrete-Time Signal Processing* Upper Saddle River, NJ: Prentice-Hall.
- [7] **Madsen, S. N.** (1989).Estimating the Doppler Centroid of SAR Data.IEEE Trans. Aerosp. Electron. Syst., vol. 2, pp. 134-140.
- [8] **Yu, W., Zhu, Z.** (1997).Comparison of Doppler Centroid Estimation Methods in SAR.In Proc. IEEE Nat. Conf., vol. 2, pp. 1015-1018.
- [9] **Wong, F., Cumming, I. G.** (1996).A Combined SAR Doppler Centroid Estimation Scheme Based Upon Signal Phase. IEEE Transactions on Geoscience and Remote Sensing, vol. 34, no. 3, pp. 696-707.
- [10] **Jin, M. Y.** (1996).Optimum Range and Doppler Centroid Estimation for a ScanSAR System.IEEE Transactions on Geoscience and Remote Sensing, vol. 34, no. 2, pp. 479-488.
- [11] **Young-Kyun, K., Byung-Lae, C., Young-Soo, K.** (2005). Ambiguity-Free Doppler Centroid Estimation Technique for Airborne SAR Using Radon Transform.IEEE Transactions on Geoscience and Remote Sensing, vol. 43, no. 3, pp. 715-721.
- [12] **Bamler, R.** (1991).Doppler Frequency Estimation and the Cramer-Rao Bound.IEEE Transactions on Geoscience and Remote Sensing, vol. 29, no. 3, pp. 385-389.
- [13] **Bamler, R., Runge, H.** (1991).PRF-Ambiguity Resolving by Wavelength Diversity.IEEE Transactions on Geoscience and Remote Sensing, vol. 29, no. 6, pp. 997-1003.

CURRICULUM VITAE



Name Surname: Pelin TUNÇAY
Place and Date of Birth: Altındağ / Turkey- 23.05.1987
Address: Hafız Ata Sokak, Ayık Apt. No:5
Daire:6Şişli/Mecidiyeköy İstanbul/Turkey
E-Mail: pelinozmn@gmail.com
B.Sc.: Eskişehir Osmangazi University
M.Sc.: Istanbul Technical University

Professional Experience and Rewards:

- Spy 2010 Savronik Project Competition, Eskişehir/Turkey - 2nd Prize
With the project: Design and control of a mobile robot using live image data taken from a stationary camera mounted at a stationary place

List of Publications and Patents:

- A.H.Tunçay, P.Özmen, "An Image Processing Based Approach for Development of Anatomically Realistic Breast Phantoms with Accurate Dielectric Properties," 1st National EMC Conference, 14-16 September 2011, Doğu University, Istanbul.
- A. H. Tunçay, P. Tunçay, İ. Akduman, "3-D Reconstruction of the Breast Surface for Microwave Breast Cancer Imaging Applications," Progress in Electromagnetics Research Symposium Abstracts, Stockholm, Sweden, August 11-15, pp. 1448, 2013.

PUBLICATIONS/PRESENTATIONS ON THE THESIS

- Tuncay, P.; Kartal, M., "A new method for Doppler centroid estimation based on block processing," *Recent Advances in Space Technologies (RAST), 2013 6th*

International Conference on , pp.417,420, 12-14 June 2013 doi: 10.1109/
RAST.2013.6581243